Received: 29 December 2017 | Revised: 23 February 2018 | Accepted: 26 February 2018
DOI: 10.1002/ardp.201700403

FULL PAPER

DPhG ARCH PHARM
Archiv der Pharmazie

Design, synthesis, and molecular modeling of heterocyclic bioisostere as potent PDE4 inhibitors

Aya M. Almatary[1,2] | Mohammad A. Elmorsy[1] | Walaa M. El Husseiny[1] | Khalid B. Selim[1] | Magda A.-A. El-Sayed[1]

[1] Faculty of Pharmacy, Department of Pharmaceutical Organic Chemistry, Mansoura University, Mansoura, Egypt

[2] Faculty of Pharmacy, Department of Pharmaceutical Chemistry, Horus University, New Damietta, Egypt

Correspondence
Dr. Magda A.-A. El-Sayed, Faculty of Pharmacy, Department of Pharmaceutical Organic Chemistry, Mansoura University, Mansoura 35516, Egypt.
Email: magdaaziz1@yahoo.com

Funding information
Research Unit, Mansoura University

Abstract

A new hybrid template was designed by combining the structural features of phosphodiesterase 4 (PDE4) inhibitors with several heterocyclic moieties which present an integral part in the skeleton of many apoptotic agents. Thirteen compounds of the synthesized hybrids displayed higher inhibitory activity against PDE4B than the reference drug, roflumilast. Further investigation indicated that compounds **13b** and **20** arrested the cell cycle at the G2/M phase and the pre-G1 phase, and induced cell death by apoptosis of A549 cells in a caspase-dependent manner.

KEYWORDS
apoptosis, caspase, cell cycle arrest, phosphodiesterase 4

1 | INTRODUCTION

A phosphodiesterase (PDE) is an enzyme that breaks a phosphodiester bond in cAMP and cGMP. It is a family of at least 11 known distinct types (PDE1 to PDE11). PDE4 is the primary enzyme that regulates the turnover of cAMP.[1] PDE4 consists of four isoforms: PDE4A, 4B, 4C, and 4D. Among the four isoforms, the PDE4B plays a key role in inflammatory cell regulation and its inhibition suppresses TNF-α production via elevation of cAMP levels.[2] The inhibition of PDE4D on the other hand triggers the emetic response.[3] Thus, selective inhibition of PDE4B was thought to provide a means to achieve efficacy while mitigating the adverse effects of the current PDE4 inhibitors. However, in spite of innumerable efforts, only a few PDE4B selective inhibitors have been reported till date.[4–7]

While PDE4 has been the target of several inflammatory diseases including COPD and asthma,[8–10] recent studies have indicated that inhibition of PDE4 isoforms raises the levels of intracellular cAMP, induces apoptosis, causes cell cycle arrest in a broad spectrum of tumor cells, and regulates the tumor microenvironment.[11–14] For example, rolipram (**1**) and roflumilast (**2**) have been proven to have the ability to attenuate lung carcinogenesis in benzo(a)pyrene-induced murine lung cancer model in mice.[15,16] Moreover, PDE4 inhibitors have been reported to induce apoptosis in several lymphoid malignancies.[17–19] Interestingly, in pancreatic cancer cell lines that are resistant to most chemotherapeutic drugs, PDE4 inhibitors reduce cellular proliferation and increase apoptosis in a caspase-dependent manner.[20]

1.1 | Rationale of the molecular design

As shown in Figure 1, the structural analysis of many PDE4 inhibitors (**1**–**4**) has identified two common features. First, the planar dialkoxyphenyl structure (marked in blue) which is tightly held in the active site by a pair of hydrophobic residues forming a hydrophobic clamp and hydrogen bond (H bond) interactions with an invariant glutamine residue that is essential for nucleotide recognition and selectivity. Second, large heterocyclic substituent (marked in red) that could form more favorable interactions with residues lining the relatively large M pocket[21,22] (Figure 2).

These findings have encouraged us to use the molecular hybridization approach, which involves the coupling of the pharmacophoric features of PDE4 inhibitors and relatively large heterocyclic moieties, in order to potentiate the PDE4 inhibitory activity and the apoptotic effect of such inhibitors.

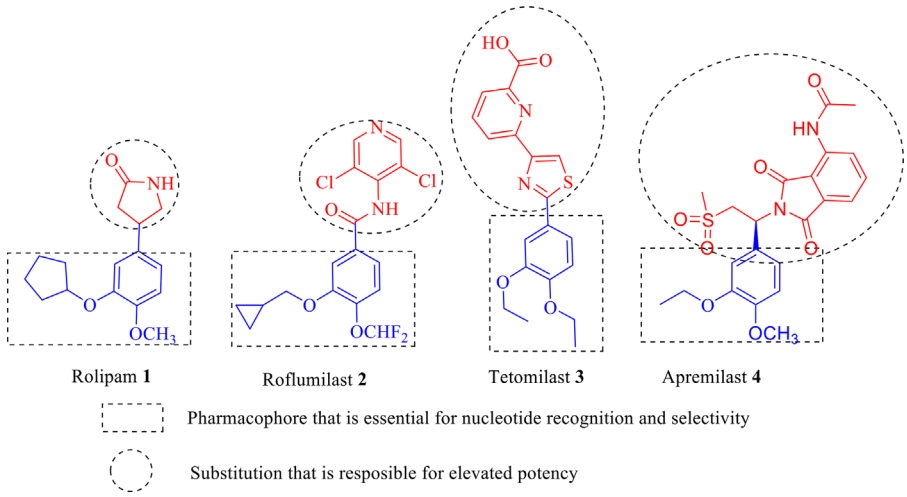

FIGURE 1 Basic pharmacophoric features of PDE4 inhibitors

In the current work, 1-(cyclopentyloxy)-2-methoxybenzene nucleus was hybridized with five important heterocyclic moieties (Figure 3). For Schemes 1 and 2, we chose the pyrimidine ring as it is archived to be incorporated in many apoptotic agents[23–25] and PDE4 inhibitors such as compound **5**.[26] Thiazole and thiazolidinone rings were chosen for Scheme 3 as they are known classes of prospective drug-like molecules, especially in the design of new anticancer/apoptotic agents.[27–31] In addition, the thiazole ring participates in the PDE4 inhibitory activity of tetomilast (**4**) and compound **6**.[32] The antitumor activity of pyran compounds has received considerable attention among researchers because of their apoptotic activity against numerous types of cancers.[33–35] The pyran nucleus has been also reported to have PDE4 inhibitory activity as shown in compound **7** (IC_{50} values = 0.1–1 μM). So that, 4-*H* pyran nucleus has been chosen for Scheme 4.[36]

2 | RESULTS AND DISCUSSION

2.1 | Chemistry

2.1.1 | Scheme 1

The key intermediate **9** was successively obtained through *O*-alkylation of isovanillin (**8**) with cyclopentyl bromide in the presence of K_2CO_3 and tetrabutylammonium bromide (TBAB) in THF. TBAB exhibited good behavior as phase transfer catalyst through environmentally friendly procedure under mild condition.[37,38]

The 6-aryl-5-cyano-2-thiouracil **10** was prepared via reaction of aldehyde **9**, ethyl cyanoacetate, and thiourea in ethanol under prolonged heating and in the presence of K_2CO_3.[39] Compound **10** was reacted with an appropriate alkyl halide in DMF to give compounds **11a–g**.[40] It is worthy to mention that the alkyl halides were reacted, by nucleophilic substitution reaction, with the hydrosulfide ion while the propargyl bromide was reacted with both the hydrosulfide ion and the nitrogen ion of the amide group due to the high reactivity of propargyl bromide. The obtained products **11a–g** were purified by column chromatography and characterized by spectral analysis (NMR and IR). For example, ^{1}H NMR spectrum of compound **11b** showed the non-equivalent allylic protons of the CH_2 group at 5.22 and 5.36 ppm as doublets and the CH allylic proton at 5.96 ppm as doublet of doublet of triplet. While in ^{13}C NMR spectrum, the carbons of CH_2 and CH groups appeared at 119.47 and 133.60 ppm, respectively.

2.1.2 | Scheme 2

The extended chain analogues **13a–h** were prepared by reacting the thiouracil derivative **10** with hydrazine hydrate to afford compound **12**

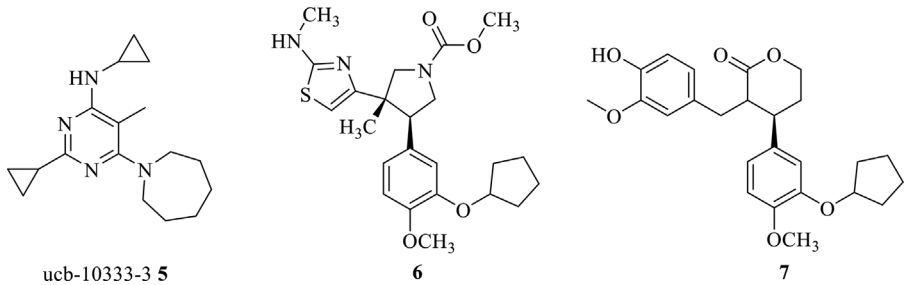

FIGURE 2 Heterocyclic compounds with PDE4 inhibitory activity

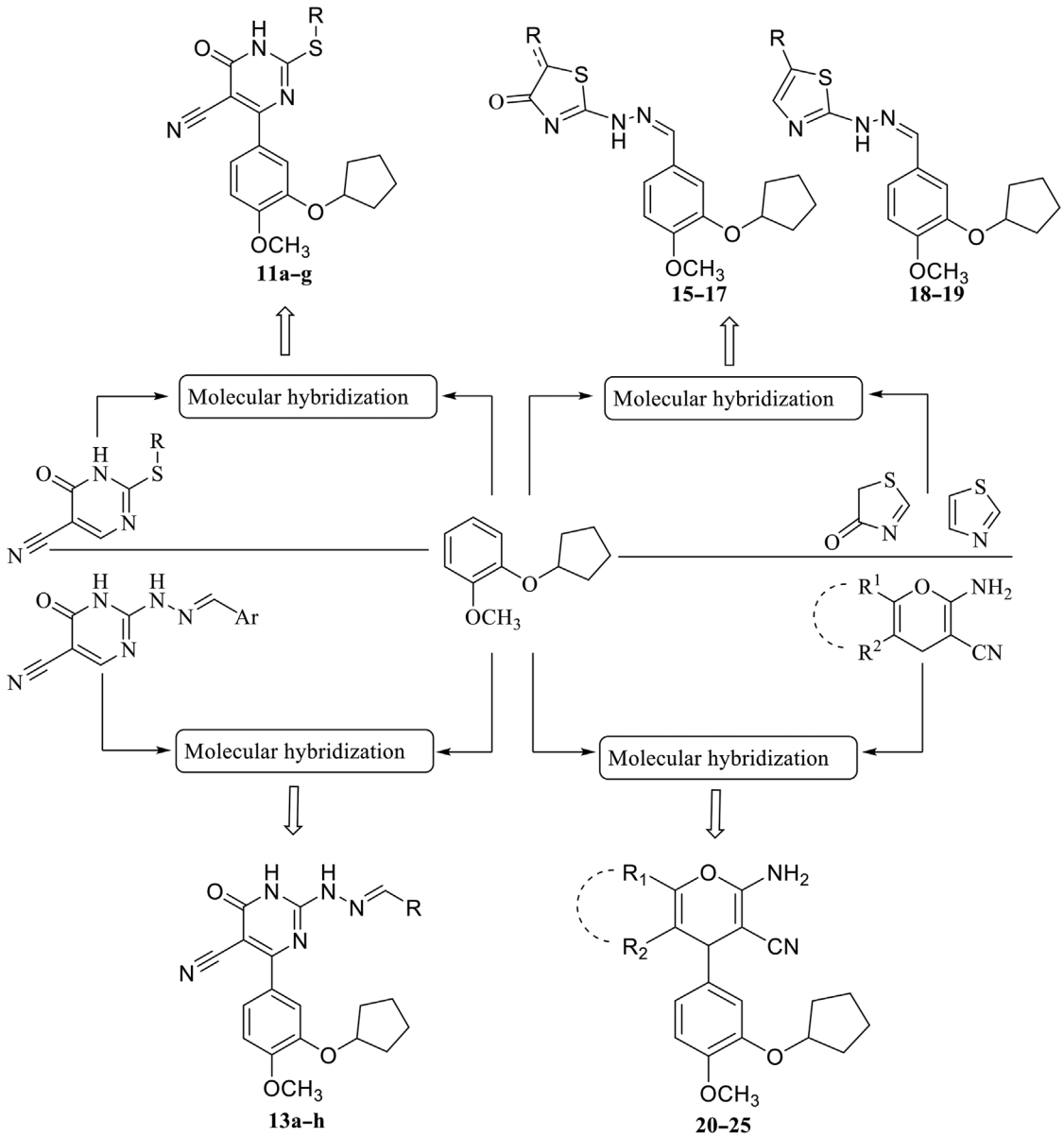

FIGURE 3 Molecular hybridization between pharmacophoric moiety of PDE4 inhibitors and several heterocyclic moieties

which was followed by reaction with different aromatic aldehydes.[41] The structure of **12** was confirmed by IR spectrum which showed bands at 3445, 3327 cm^{-1} corresponding to NH_2, NH groups, while the ^1H NMR spectrum confirmed the presence of their protons with signals at 2.4 and 11.3 ppm, respectively. The presence of the imine group in Schiff bases **13a–h** was observed by IR spectra with stretching vibration at 1606–1661 cm^{-1} and by ^1H NMR spectra with singlet signal of CH═N group at 8–8.9 ppm and doublet signal of N—NH group at 11.5 ppm.

2.1.3 | Scheme 3

The thiosemicarbazone derivative **14** was obtained through a condensation reaction between aldehyde **9** and thiosemicarbazide (TSC). The obtained thiosemicarbazone **14** was used to prepare 4-thiazolidinones series which is substituted at the five position with different groups. Reaction of **14** with ethyl chloroacetate in glacial acetic acid and in the presence of a catalytic amount of sodium acetate afforded the corresponding 4-thiazolidinone derivative **15**.[42] Since the presence of an acid function introduces an additional diversity point and further structural tuning, we utilized a thia-Michael addition reaction with the employment of maleic anhydride as the acceptor of Michael to give compound **16**. The reaction was carried out in dry toluene and DMF.[43] Treatment of **14** with dimethyl acetylenedicarboxylate (DMAD) afforded compound **17**.[42] IR spectrum of compound **17** showed characteristic absorption band at 1727, 1702 cm^{-1} corresponding to carbonyl groups. Also, the ^1H NMR spectrum revealed singlet signal at 3.8 ppm corresponding to CH_3 of the ester and signal at 6.6 ppm corresponding to CH═N. The Hantzsch reaction of thiosemicarbazone derivative with some α-halocarbonyl

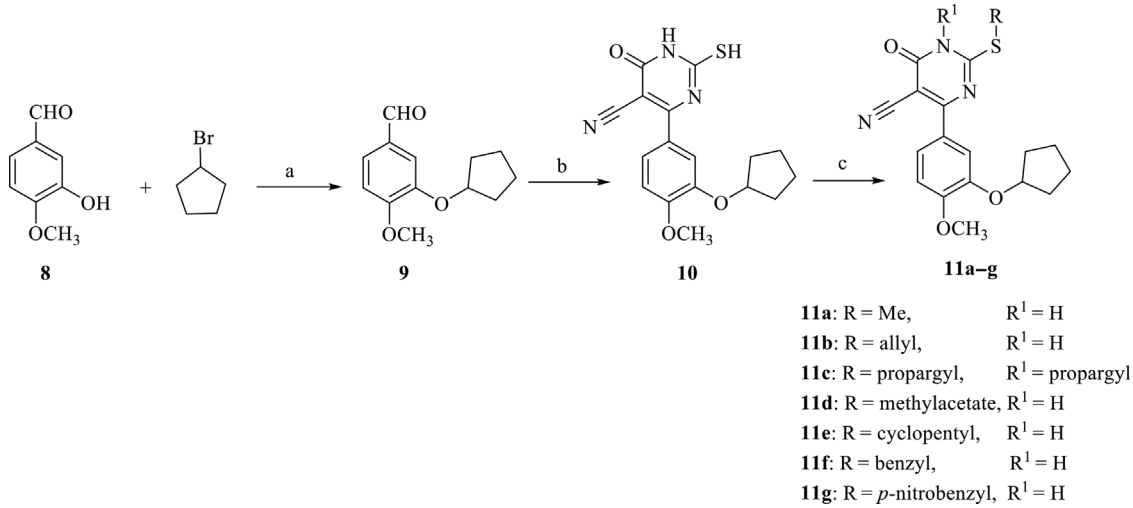

SCHEME 1 Reagents and conditions: (a) TBAB, K_2CO_3, THF, reflux, 12 h; (b) thiourea, ethyl cyanoacetate, K_2CO_3, absolute ethanol, reflux 10 h; (c) appropriate alkyl halide, K_2CO_3, DMF, reflux, 10 h

compounds was investigated to synthesize versatile thiazole derivatives. Cyclocondensation of thiosemicarbazone **14** with ethyl-4-chloroacetoacetate in ethanol resulted in the formation of compound **18**.[42] The ^{1}H NMR spectrum of **18** exhibited a triplet signal at 1.2 ppm characteristic for CH_3 protons and a quartet signal at δ 4.14 ppm for CH_2 protons of the ester group. Furthermore, **14** was reacted with different phenacyl bromides under the same reaction conditions to produce 1,3-thiazoles derivatives **19a–c**. Notably, the reactions were completed within 15–30 min affording the expected products **19a–c** in good yields. We were delighted to observe such a quick reaction rate in some of the cases without using any additives and/or ligands or microwave or ultrasound.

2.1.4 | Scheme 4

The Knoevenagel condensation between compound **9** and malononitrile was carried out directly in absolute ethanol to give the arylmethylene-malononitrile **20**. The reaction of derivative **20** and C—H activated compounds was carried out by standard Michael addition in the usual mild basic conditions to give compounds **21–24**.[44,45] The ^{1}H NMR spectra of the products revealed the characteristic singlet signal of the *H*-pyran at 4.5–4.8 ppm and the two protons of the NH_2 group at 6.5–6.8 ppm. Domino's Knoevenagel condensation/Michael of compound **9**, malononitrile and dimedone in presence of TBAB was performed and gave compound **25**.[46]

2.2 | Evaluation of biological activity

2.2.1 | PDE4B enzyme inhibition assay

Enzyme assay was used to measure the IC_{50} values of the PDE4B inhibition of the synthesized compounds along with roflumilast as a reference drug and the results are presented in Table 1. It is worthy to mention that 13 of the newly synthesized compounds showed improved inhibition of PDE4B over roflumilast. It is evident from Table 1 that compounds **13b** and **20** showed excellent inhibition (<2-fold over the reference). Compounds **24** and **13c** were found to be next best. Compound **13h** was found to be the least active in these series (Figure 4).

Our investigation into the SAR of our compounds revealed that the majority of the synthesized compounds of Scheme 1 showed moderate to weak activity in comparison with roflumilast. The only

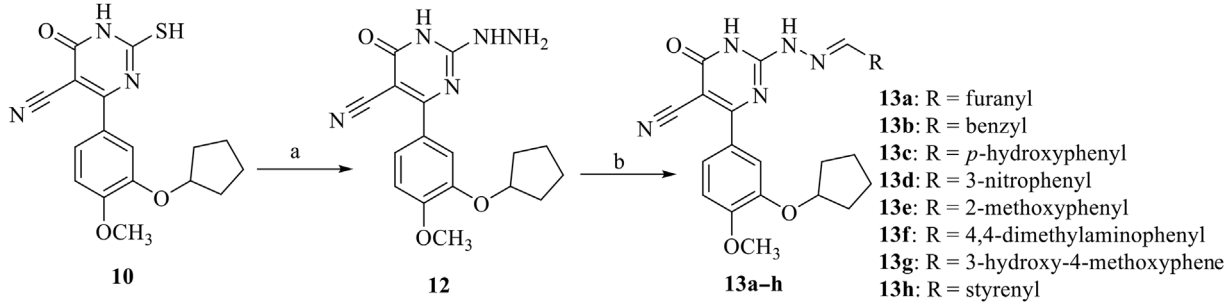

SCHEME 2 Reagents and conditions: (a) Hydrazine hydrate, absolute ethanol, reflux, 12 h; (b) appropriate aromatic aldehyde, absolute ethanol, reflux, 10 h

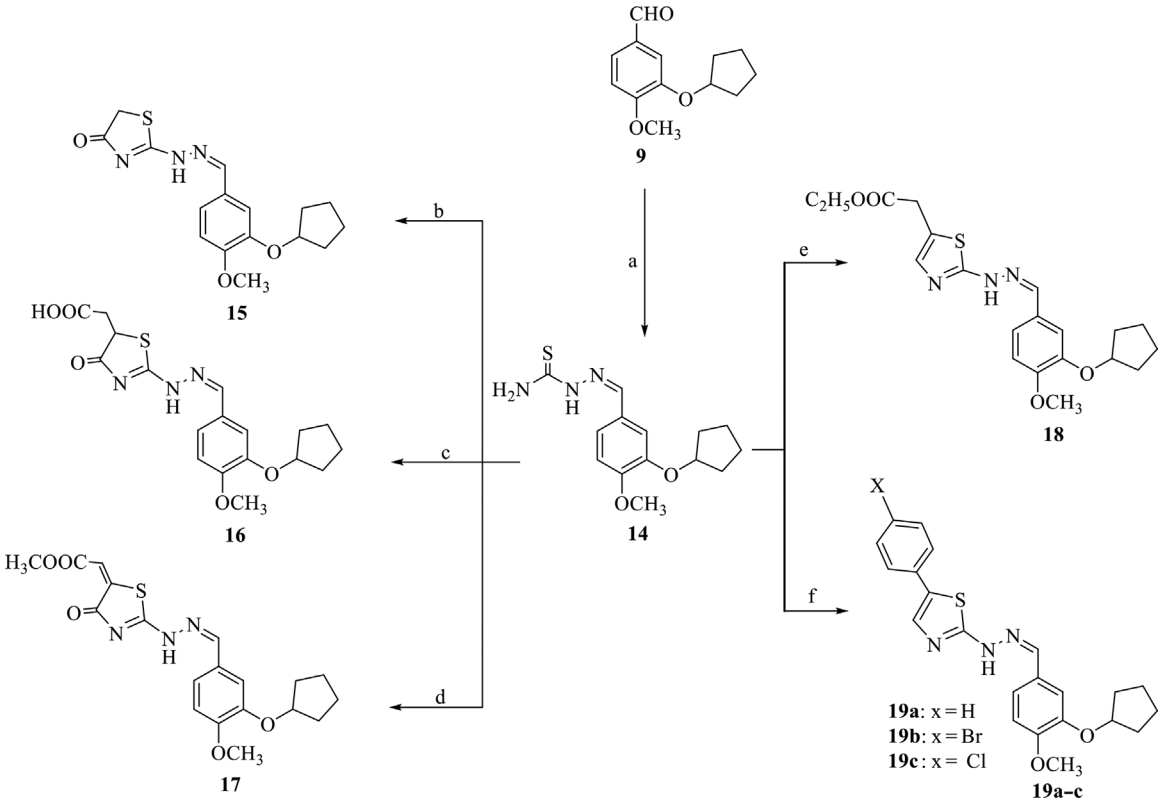

SCHEME 3 Reagents and conditions: (a) TSC, absolute ethanol, reflux, 10 h; (b) ethyl chloroacetate, NaOAc, acetic acid, reflux, 10 h; (c) maleic anhydride, toluene/DMF (25:1), reflux, 12 h; (d) DMAD, absolute ethanol, reflux, 1 h; (e) ethyl 4-chloroacetoacetate, absolute ethanol, reflux, 10 h; (f) appropriate phenacyl bromide, absolute ethanol, reflux, 0.5 h

exception was compound **11d** with IC_{50} value of 47 nM that exceeds the reference compound.

On the other hand, the insertion of the azomethine spacer in compounds **13a–h** resulted in powerful improvement of the inhibitory activity compared with the corresponding pyrimidine derivatives **11a–g** of Scheme 1, suggesting that the azomethine spacer may play an important role in potentiating the activity. The replacement of furanyl substitution with benzyl substitution has resulted in a twofold increase in the inhibitory activity of compound **13b** with IC_{50} value of 27 nM. It was apparent that any further substitution of the benzyl ring resulted in a slight loss of the IC_{50} values. Moreover, we can notice that the size of the substituent has a noticeable effect on the activity as a gradual decrease in PDE4B inhibitory activity was observed in conjunction with the increase of the size of the substituents. It was noticed also that any increase in the length of the azomethine spacer will result in a dramatic drop in the inhibitory activity as observed in compound **13h** with IC_{50} value of 352 nM.

In completion of the SAR study analysis, the hybridization of the catechol diether moiety with the thiazole and the thiazolidinone rings in presence of the azomethine spacer in between also showed an excellent inhibitory activity on PDE4B. Starting with the thiazolidinone derivatives, it was noticed that in contrast to Scheme 2 as the size of the substitution increases the inhibitory activity increases. For example, compound **17** with the ester substitution at 4-position showed the highest inhibitory activity with IC_{50} value of 48 nM, comes next compound **16** with the carboxylate functionality with IC_{50} value of 50 nM. Compound **15** (with no substitution) showed a tremendous drop in the inhibitory activity with IC_{50} value of 259 nM. Careful analysis on the SAR of the thiazole derivatives revealed that the introduction of the phenyl moiety resulted in increased activity of compound **19a–c** (IC_{50} from 46 μM to 52 nM) when compared to compound **18** (IC_{50} = 262 nM).

Interestingly, the starting material for Scheme 4, 2-(3-(cyclopentyloxy)-4-methoxybenzylidene) malononitrile (**20**) bearing the double cyano groups, played the highest PDE4B inhibitory activity in Scheme 4 and comes next in the inhibitory activity of all compounds. Analysis of the structure–activity relationship of compounds **21–25** revealed that the size of the pyran substituent has a noteworthy effect on the activity. For example, the insertion of the methyl group and the increase in the size of the ester group in compound **22** (IC_{50} = 56 nM) has resulted in threefold increase in the inhibitory activity more than compound **21** (IC_{50} = 139 nM). Furthermore, the same attitude was observed in the pyran derivatives **23–25** as compound **24** (naphthyl substitution) has IC_{50} value of 39 nM, comes next compound **23** (phenolic substitution) and compound **25** (cyclic ketone substitution) with IC_{50} values of 74 and 99 nM, respectively.

From the SAR study of our compounds **10–25**, we concluded that as the size of the dialkoxyphenyl substitution increases, the PDE4B inhibitory activity increases to a specific size limit after which a drop in the activity will be observed.

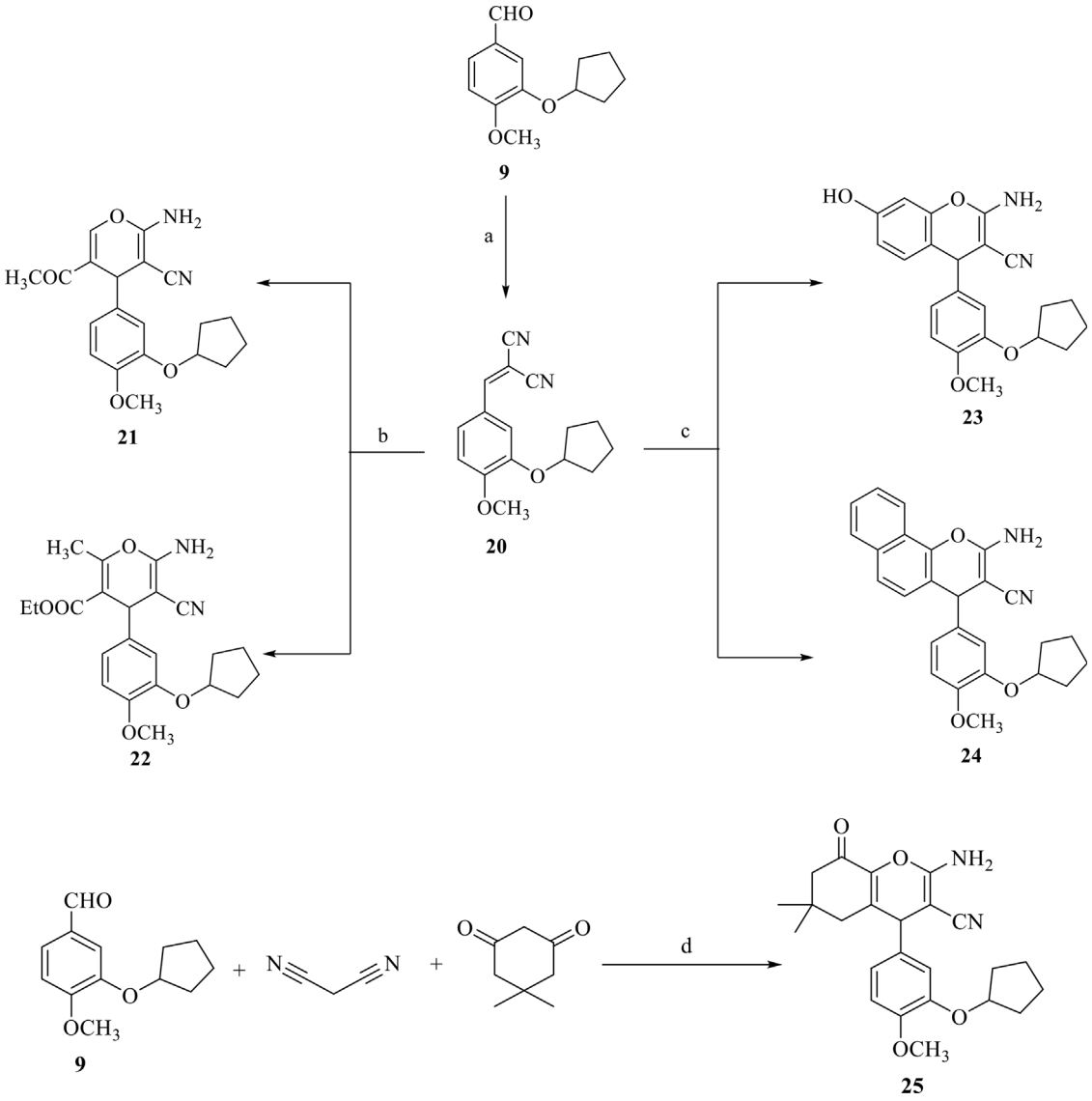

SCHEME 4 Reagents and conditions: (a) Malononitrile, absolute ethanol, reflux, 12 h; (b) appropriate β-dicarbonyl compound, piperidine, dry ether, stirring, 2 h; (c) appropriate phenol, piperidine, toluene, reflux, 10 h; (d) TBAB, absolute ethanol, reflux 12 h

2.2.2 | Apoptosis assay

The apoptotic effect was measured with Annexin V-FITC/PI double staining and quantitated by flow cytometry whereas 5-FU was included as a reference compound. As shown in Figure 5, the apoptotic cell population was significantly increased in the presence of compounds **13b** (from 0.85 to 9.79%) and **20** (from 0.85 to 5.76%).

2.2.3 | Cell cycle analysis

Compounds **13b** and **20** were subjected to a cell-cycle distribution assay by treating A549 cells with both compounds. Propidium iodide (PI) staining data revealed that upon exposure of the cells to IC_{50} concentration of our compound against A549 cells, the cell number at G2/M and pre-G1 phase was substantially increased. In case of compound **13b**, the cell number increased from 6.2 to 14.22% in G2/M phase and from 0.92 to 11.08% in pre-G1 phase. Whereas, the cell number in case of compound **20** was increased from 6.2 to 10.88% in G2/M phase and from 0.92 to 6.65% in pre-G1 phase. The results suggested that both compounds induced an obvious cell-cycle arrest at G2/M phase and apoptosis at pre-G1 phase (Table 2 and Figure 5).

2.2.4 | Detection and quantification of the levels of human active caspase-3 and -9 proteins

To further clarify the specific signaling pathway involved in the apoptotic effects of our compounds, we evaluated the appropriate protein expression patterns using human Caspase-3 and -9 ELISA, which is an enzyme-linked immunosorbent assay for the quantitative detection of human caspase-3 and -9. As shown in Table 2, expression of cleaved caspase-3 and -9 was markedly increased upon treatment with compounds **13b** and **20**. Caspase-3 concentration was elevated

TABLE 1 Inhibitory activity of target compounds against PDE4B

Scheme 1		Scheme 2		Scheme 3		Scheme 4	
Comp.	IC_{50}[a] (nM)	Comp.	IC_{50} (nM)	Comp.	IC_{50} (nM)	Comp.	IC_{50} (nM)
10	160 ± 0.12	**12**	44 ± 0.02	**14**	188 ± 0.11	**20**	33 ± 0.02
11a	236 ± 0.14	**13a**	47 ± 0.02	**15**	259 ± 0.17	**21**	139 ± 0.12
11b	84 ± 0.03	**13b**	27 ± 0.01	**16**	50 ± 0.02	**22**	53 ± 0.04
11c	N.D.[b]	**13c**	43 ± 0.01	**17**	48 ± 0.01	**23**	74 ± 0.03
11d	47[c] ± 0.01	**13d**	46 ± 0.01	**18**	262 ± 0.13	**24**	39 ± 0.02
11e	62 ± 0.04	**13e**	156 ± 0.2	**19a**	46 ± 0.02	**25**	99 ± 0.07
11f	177 ± 0.11	**13f**	79 ± 0.04	**19b**	51 ± 0.02	Roflumilast	52 ± 0.03
11g	218 ± 0.092	**13g**	98 ± 0.05	**19c**	52 ± 0.04		
		13h	352 ± 0.19				

[a]Data are presented as the means ± SDs of four independent experiments.
[b]N.D.: not determined.
[c]Underlined IC_{50} values showed more potent inhibitory activity than roflumilast.

from 0.053 to 0.617 ng/mL for compound **13b** and to 0.526 ng/mL in case of compound **20**. Furthermore, caspase-9 concentration was elevated from 0.1726 to 16.91 ng/mL for compound **13b** and to 15.39 ng/mL in case of compound **20**.

2.3 | Molecular docking study

To understand the basis for PDE4B inhibitory activity, we pursued a molecular docking study with compounds that showed the highest inhibitory activity. In this investigation, the 3D structure of PDE4B was taken from a Protein Data Bank entry (PDB entry 1XMU) having the ligand roflumilast in place. The new inhibitors were built and optimized at the ChemDraw professional 2016. The resulting structures were then docked and analyzed by MOE software to identify specific contacts between ligands and receptor.

Initially, we selected three of the most potent compounds **12**, **13a**, and **13b** for the docking experiments. The active site of the PDE4B catalytic domain is divided into three pockets: the metal binding pocket (M), the purine selective glutamine, and hydrophobic clamp pocket (Q) which is further divided into Q1 and Q2 subpockets and the solvent-filled side pocket (S). Figure 6 depicts a schematic binding profile of these compounds. This docking orientation revealed the catechol diether as the key pharmacophore. The methoxy group binds at the Q_1 pocket, while the cyclopentyl ether group binds at the Q_2 pocket. These two substituents seem to be optimized for maximum interactions with residues in the Q_1 and Q_2 pockets. The heterocyclic group extends to the dimetal ion site and forms one H bond to a water molecule that is coordinated to Mg^{2+}.

Looking closely, we will observe that the methoxy group forms integral hydrogen bonds with the conserved glutamine residue (Gln443). The phenyl moiety was also notably positioned between the Phe446, Phe414, and isoleucine (Ile410), which formed the cavity accommodating the hydrophobic moiety of the compounds.

Compared to roflumilast, compounds **12**, **13a–13d** adopted the same alignment in the purine-selective glutamine and hydrophobic clamp pockets (Q1 and Q2) with subtle apparent variances. Figure 7

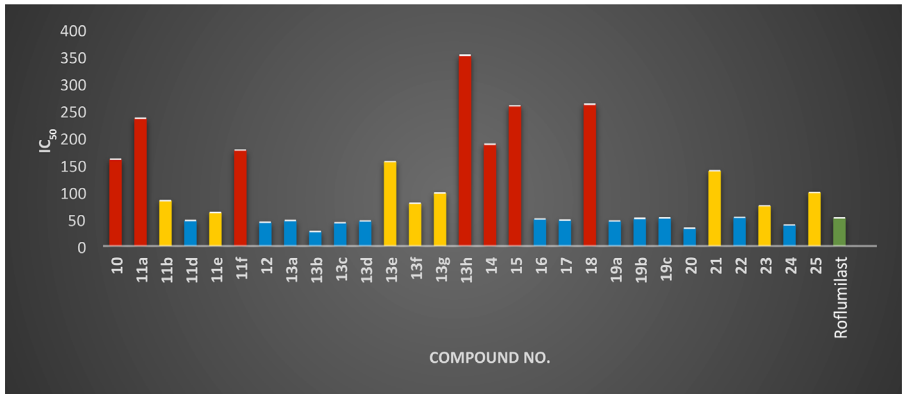

FIGURE 4 Bar chart representing the IC_{50} values of the tested compounds against PDE4B compared with roflumilast as reference, with error bar included

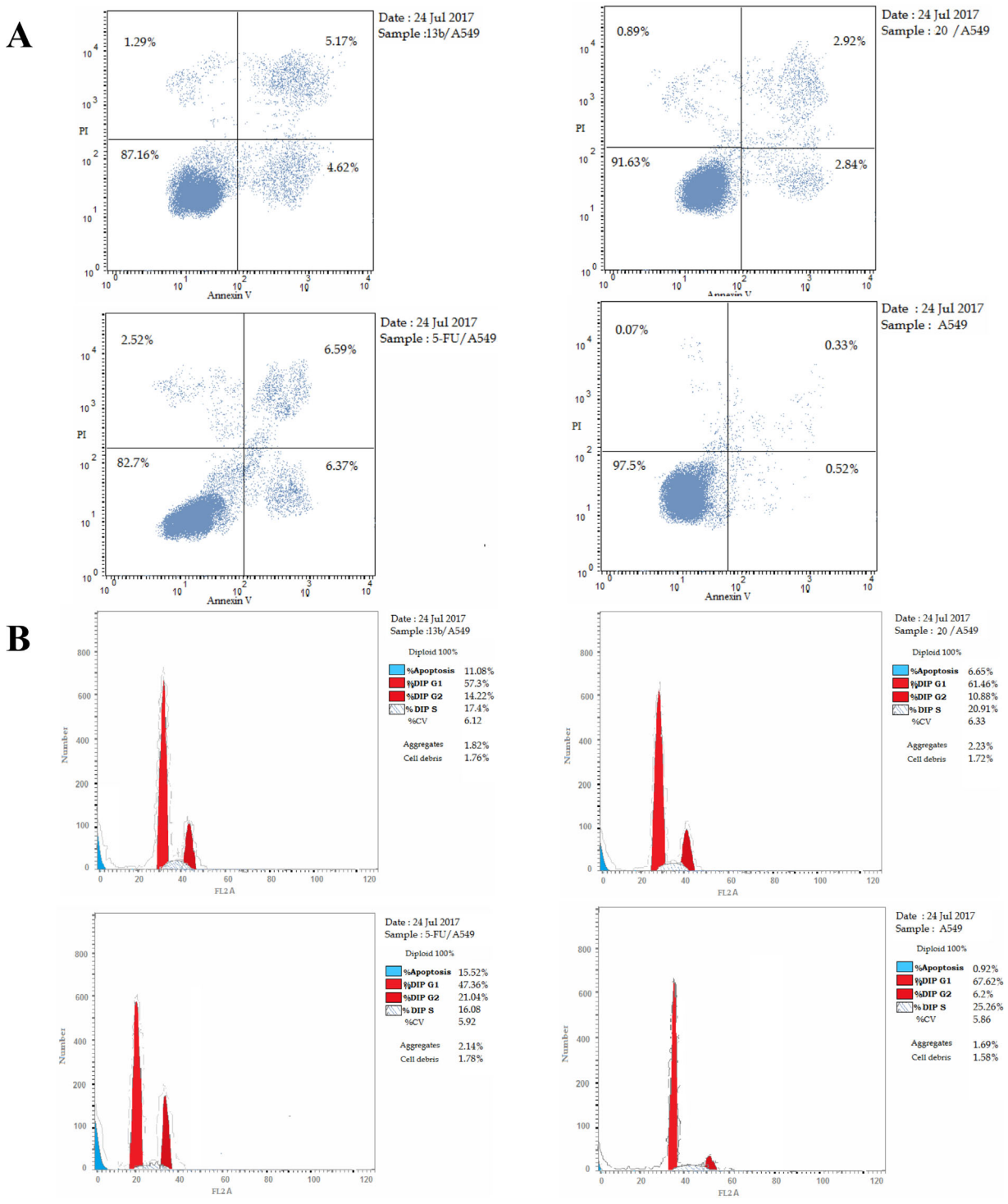

FIGURE 5 Determination of apoptosis in A549 cell line via Annexin V/PI staining and cell cycle arrest with flow cytometry. (A) Cells were stained with FITC-conjugated Annexin V and PI after induction of apoptosis and monitored using flow cytometry. (B) A549 cell line was treated with compounds **13b** and **20** for 24 h, then subjected to propidium iodide (PI) staining and flow cytometry

presents the docking conformations of roflumilast (purple), **12** (white), **13a** (green), **13b** (light blue), **13c** (orange), and **13d** (gray) in the active site of PDE4B. The docking scores and molecular interactions of compounds **12**, **13a–13d** after docking into the PDE4B protein are presented in Table 3. It is evident that nearly all of these compounds showed a higher docking score than roflumilast. Additionally, all of these compounds showed favorable interactions with glutamine residue that is essential for nucleotide recognition but not roflumilast. These two reasons are probably the main causes of the higher PDE4B inhibitory activity of our compounds than roflumilast.

TABLE 2 Cell cycle arrest analysis and caspase-3 and -9 detection and quantification

	Caspase-3			Caspase-9			Cell cycle arrest (μM/mL)			
Comp.	Conc.[a] μM	Casp.3[b] conc. ng/mL	Fold	Conc.[a] μM	Casp.9 conc. ng/mL	Fold	%G0-G1	%S	%G2-M	%Pre-G1
13b	2.36 ± 0.25	0.617	11.55	2.36	16.91	97.9	57.3	17.4	14.22	11.08
20	3.29 ± 0.11	0.526	9.84	3.29	15.39	89.16	61.46	20.91	10.88	6.65
5-FU	1.85	0.582	10.89	7.4	16.84	97.5	47.36	16.08	21.04	15.52
Cont.		0.053	1		0.1726	1	67.62	25.26	6.2	0.92

[a]Concentration used for the determination of caspase-3 and -9 and the cell cycle arrest analysis was equal to the IC_{50} against A549 cell line of each compound.
[b]Casp.: Caspase: Cysteinyl aspartate-specific proteinase.

3 | CONCLUSION

In conclusion, a new hybrid template has been designed by integrating the pharmacophoric (dialkyloxyphenyl) moiety of PDE4 inhibitors with several heterocyclic rings. The synthesized hybrids displayed a high inhibitory activity against PDE4B and 13 of them exceeded the activity of roflumilast. Further investigation indicated that compounds **13b** and **20** arrested cell cycle at the G2/M phase and pre-G1 phase and induced cell apoptosis in A549 cells through caspase-dependent manner.

4 | EXPERIMENTAL

4.1 | Chemistry

4.1.1 | General

Reagents and solvents were purchased from commercial sources and were used without further purification. Reaction times were determined using TLC technique on silica gel plates 60 F_{245} E. Merck, and the spots were visualized by UV light (366, 245 nm). Melting points were determined on Stuart melting point apparatus and are uncorrected. ^{1}H NMR and ^{13}C NMR spectra were recorded on a JEOL 500 and 125 MHz spectrometer, respectively. IR spectra were recorded on a Nicolet iS10 infrared spectrometer. Compound **9** was synthesized according to the reported procedure.[38]

The NMR spectra of the compounds synthesized by Schemes 1, 2, and 4 are provided as Supporting Information. The InChI codes of the investigated compounds as well as some biological activity data are also provided as Supporting Information.

4-(3-(Cyclopentyloxy)-4-methoxyphenyl)-2-mercapto-6-oxo-1,6-dihydropyrimidine-5-carbonitrile (10)

A mixture of compound **9** (0.22 g, 1 mmol), ethylcyanoacetate (0.113 g, 1 mmol), thiourea (0.076 g, 1 mmol), and potassium carbonate (0.138 g, 1 mmol), were refluxed in ethanol for 10 h. Upon completion of the reaction as judged by TLC, the formed solid was filtered, washed with THF, and then dried. The dry solid was dissolved in water and stirred at 80°C for 30 min till the solid is completely dissolved. Acidify with acetic acid till the pH is 5 as judged by pH meter, continue stirring on cold. The formed solid was filtered and recrystallized from ethanol. Yield 63.6%. Pale yellow solid. Mp: 190–191°C. IR (KBr, cm^{-1}) 3570 (NH), 3503 (SH), 2962 (aliph. CH), 2229 (CN), and 1658 (CO). ^{1}H NMR (500 MHz, DMSO-d_6, δ, ppm) δ 11.56 (s, 1H), 7.40 (dd, J = 8.5, 2.1 Hz, 1H), 7.37 (d, J = 2.1 Hz, 1H), 7.04 (d, J = 8.5 Hz, 1H), 4.84–4.68 (m, 1H), 3.80 (s, 3H), 2.06–1.48 (m, 8H). Elemental analysis for $C_{17}H_{17}N_3O_3S$, calcd.: C, 59.46; H, 4.99; N, 12.24. Found: C, 59.48; H, 5.10; N, 12.25.

4.1.2 | General procedure for the synthesis of compounds 11a–g

A mixture of compound **10** (0.343 g, 1 mmol), alkyl halides (1 mmol), and potassium carbonate (0.138 g, 1 mmol) were refluxed in DMF for 12 h. Upon completion of the reaction as judged by TLC, the reaction mixture was poured into water acidified with 5 N HCL. The formed solid was stirred for 15 min then filtered and washed with water. The products were purified by column chromatography.

4-(3-(Cyclopentyloxy)-4-methoxyphenyl)-2-(methylthio)-6-oxo-1,6-dihydropyrimidine-5-carbonitrile (11a)

It was purified with column chromatography (CH_2Cl_2/MeOH 9:1). Yield 66%. White solid. Mp: 260–261°C. IR (KBr, $cm^{-1)}$ 3423 (NH), 2955 (aliph. CH), 2216 (CN), 1650 (CO). ^{1}H NMR (500 MHz, DMSO-d_6, δ, ppm) δ 7.40 (dd, J = 8.5, 2.1 Hz, 1H), 7.37 (d, J = 2.1 Hz, 1H), 7.04 (d, J = 8.5 Hz, 1H), 4.84–4.68 (m, 1H), 3.80 (s, 3H), 2.6 (s, 3H), 2.06–1.48 (m, 8H). Elemental analysis for $C_{18}H_{19}N_3O_3S$, calcd.: C, 60.49; H, 5.36; N, 11.76. Found: C, 60.51; H, 5.37; N, 11.78.

2-(Allylthio)-4-(3-(cyclopentyloxy)-4-methoxyphenyl)-6-oxo-1,6-dihydropyrimidine-5-carbonitrile (11b)

Yield 74%. Yellow solid. Mp: 200–201°C. ^{1}H NMR (500 MHz, $CDCL_3$, δ, ppm) δ 7.82 (dd, J = 8.6, 2.1 Hz, 1H), 7.71 (d, J = 2.0 Hz, 1H), 6.96 (d, J = 8.6 Hz, 1H), 5.96 (ddt, J = 16.9, 10.1, 6.8 Hz, 1H), 5.36 (d, J = 17.1 Hz, 1H), 5.22 (d, J = 10.2 Hz, 1H), 4.82 (m, 1H), 3.97 (d, J = 6.8 Hz, 2H), 3.92 (s, 3H), 2.09–1.61 (m, 8H). ^{13}C NMR (125 MHz, DMSO-d_6, δ, ppm) δ 166.70, 165.21, 161.86, 153.50, 147.22, 133.58, 127.74, 123.21, 119.47, 117.05, 115.14, 112.34, 92.04, 80.38, 56.43, 33.51, 32.91, 24.25. Elemental analysis for $C_{20}H_{21}N_3O_3S$, calcd.: C, 62.64; H, 5.52; N, 10.96. Found: C, 62.67; H, 5.53; N, 10.97.

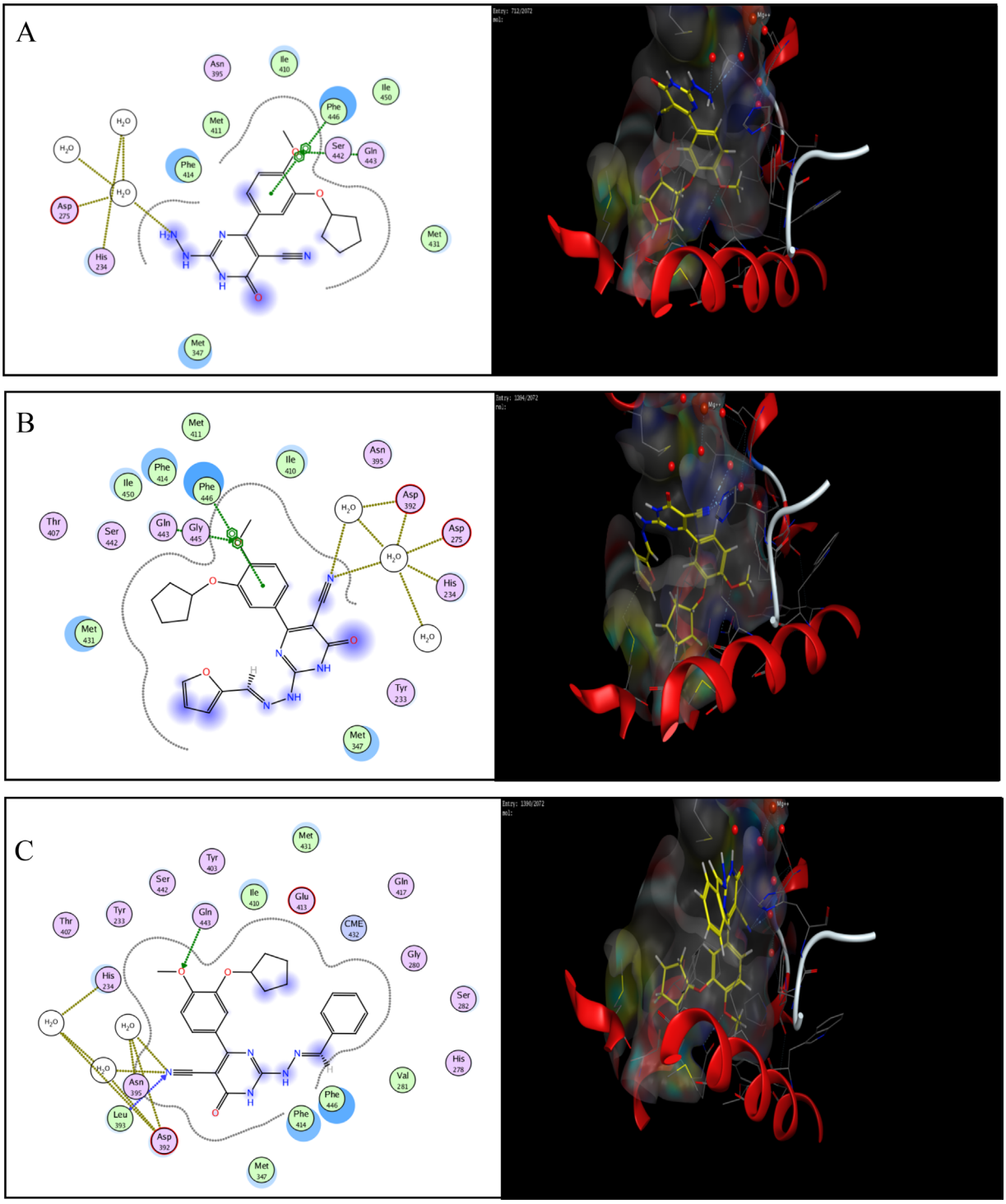

FIGURE 6 Binding mode of **12** (A), **13a** (B), **13b** (C) in the catalytic pocket of PDE4B

4-(3-(Cyclopentyloxy)-4-methoxyphenyl)-6-oxo-1-(prop-2-yn-1-yl)-2-(prop-2-yn-1-ylthio)-1,6-dihydropyrimidine-5-carbonitrile (11c)

It was purified with column chromatography (pet. ether/ethyl acetate 3:1). Yield 10%. White solid. Mp: 242–243°C. ^{1}H NMR (500 MHz, DMSO-d_6, δ, ppm) δ 7.72 (dd, J = 8.5, 2.0 Hz, 1H), 7.68 (d, J = 2.1 Hz, 1H), 7.18 (d, J = 8.6 Hz, 2H), 5.23 (d, J = 2.4 Hz, 2H), 4.84 (m, 1H), 4.10 (d, J = 2.5 Hz, 2H), 3.86 (s, 3H), 3.75 (t, J = 2.4 Hz, 1H), 3.23 (t, J = 2.4 Hz, 1H), 2.06–1.48 (m, 8H). Elemental analysis for $C_{23}H_{21}N_3O_3S$, calcd.: C, 65.85; H, 5.05; N, 10.02. Found C, 65.87; H, 5.09; N, 10.03.

Methyl-2-((5-cyano-4-(3-(cyclopentyloxy)-4-methoxyphenyl)-6-oxo-1,6-dihydropyrimidin-2-yl)thio)acetate (11d)

It was purified with column chromatography (pet. ether/ethyl acetate 3:1). Yield 33%. White solid. Mp: 192–193°C. ^{1}H NMR (500 MHz,

TABLE 3 Docking scores and summary of molecular interactions of compounds **12**, **13a–13d** after docking into PDE4B

Comp.	Docking score	Summary of interactions
12	−5.7	Gln443, Phe446, Asp275
13a	−6.9	Gln443, Phe446, Asp275, Asp392
13b	−3.3	Gln443, Leu293, Asp392
13c	−5.9	Gln443, Phe446, Gln264, Gln304, His278
13d	−7.1	Gln443, Phe446, Asp275, Asp392, His234
Roflumilast	−4.4	Thr407, Asp275, Asp392, His234

DMSO-d_6, δ, ppm) δ 7.57 (dd, J = 8.6,2.1 Hz, 1H), 7.53 (d, J = 2.1 Hz, 1H), 7.10 (d, J = 8.5 Hz, 1H), 4.85–4.75 (m, 1H), 4.12 (s, 2H), 3.80 (s, 3H), 3.58 (s, 3H), 2.06–1.48 (m, 8H). ^{13}C NMR (125 MHz, DMSO-d_6, δ, ppm) δ 169.13, 161.96, 153.49, 146.99, 123.18, 115.18, 112.33, 80.28, 56.30, 52.97, 33.14, 32.76, 24.13. Elemental analysis for $C_{20}H_{21}N_3O_5S$, calcd.: C, 57.82; H, 5.10; N, 10.11. Found: C, 57.84; H, 5.10; N, 10.12.

4-(3-(Cyclopentyloxy)-4-methoxyphenyl)-2-(cyclopentylthio)-6-oxo-1,6-dihydropyrimidine-5-carbonitrile (11e)

Yield 98%. White solid. Mp: 128–129°C. IR (KBr, cm^{-1}) 3446 (NH), 2955 (aliph. CH), 2209 (CN), 1628 (CO). ^{1}H NMR (500 MHz, $CDCl_3$, δ, ppm) δ 7.9 (dd, J = 8.5, 2.1 Hz, 1H), 7.7 (d, 2.1 Hz, 1H), 7.0 (d, J = 8.5 Hz, 1H), 4.84–4.68 (m, 1H), 4.17–4.24 (m,1H), 3.80 (s, 3H), 2.2–1.6 (m, 16H). ^{13}C NMR (125 MHz, δ, ppm) δ 174.98, 169.48, 167.73, 153.26, 147.31, 127.69, 122.89, 115.06, 112.44, 87.35, 82.01, 80.38, 56.39, 44.45, 33.36, 32.91, 25.12, 24.24. Elemental analysis for $C_{22}H_{25}N_3O_3S$, calcd.: C, 64.21; H, 6.12; N, 10.21. Found: C, 64.23; H, 6.13; N, 10.23.

2-(Benzylthio)-4-(3-(cyclopentyloxy)-4-methoxyphenyl)-6-oxo-1,6-dihydropyrimidine-5-carbonitrile (11f)

It was purified with column chromatography (pet. ether/ethyl acetate 3:1). Yield 30%. Orange solid. Mp: 253–254°C. ^{1}H NMR (500 MHz, DMSO-d_6, δ, ppm) δ 7.67 (dd, J = 8.5.2.1 Hz, 1H), 7.57 (d, J = 2.0, 1H), 7.42 (d, J = 7.2 Hz, 2H), 7.32 (t, J = 7.3 Hz, 2H), 7.27 (t, J = 7.3 Hz, 1H), 7.14 (d, J = 8.8 Hz, 1H), 4.77–4.64 (m, 1H), 4.57 (s, 2H), 3.84 (s, 3H), 2.06–1.48 (m, 8H). ^{13}C NMR (125 MHz, DMSO-d_6, δ, ppm) δ 166.70, 165.37, 153.20, 147.15, 146.96, 145.92, 130.52, 127.63, 124.08, 123.02, 117.07, 114.94, 112.14, 92.02, 80.09, 56.22, 33.64, 32.69, 24.09. Elemental analysis for $C_{24}H_{23}N_3O_3S$, calcd.: C, 66.49; H, 5.35; N, 9.69. Found: C, 66.50; H, 5.35; N, 9.71.

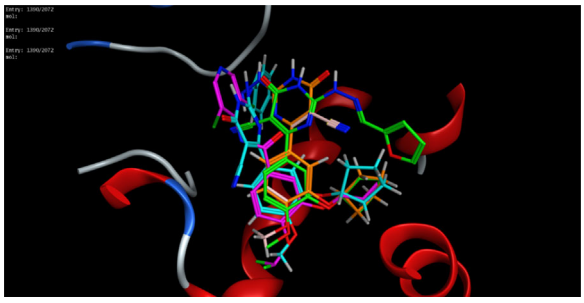

FIGURE 7 Key residues in the binding site of roflumilast (purple), **12** (white), **13a** (green), **13b** (light blue), **13c** (orange), **13d** (gray)

4-(3-(Cyclopentyloxy)-4-methoxyphenyl)-2-(4-nitrobenzylthio)-6-oxo-1,6-dihydropyrimidine-5-carbonitrile (11g)

It was purified with column chromatography (pet. ether/ethyl acetate 3:1). Yield 25%. Yellow solid. Mp: 200–201°C. IR (KBr, cm^{-1}) 3570 (NH), 3503 (SH), 2962 (alph. CH), 2229 (CN), 1658 (CO), and 1516–1377 (NO_2). ^{1}H NMR (500 MHz, $CDCl_3$, δ, ppm) δ 8.16 (d, J = 8.6 Hz, 2H), 7.70 (dd, J = 8.5,2.1 Hz, 1H), 7.63 (d, J = 2.1, 1H), 7.56 (d, J = 8.5 Hz, 2H), 6.94 (d, J = 8.6 Hz, 1H), 4.77 (m, 1H), 4.62 (s, 2H), 3.93 (s, 3H), 2.06–1.48 (m, 8H). ^{13}C NMR (125 MHz, DMSO-d_6, δ, ppm) δ 166.86, 153.37, 147.34, 147.14, 146.12, 130.71, 127.83, 124.27, 123.20, 117.27, 115.13, 112.33, 80.27, 56.41, 33.82, 32.8, 31.39, 24.27. Elemental analysis for $C_{24}H_{22}N_4O_5S$, calcd.: C, 60.24; H, 4.63; N, 11.71. Found: C, 60.26; H, 4.67; N, 11.73.

4-(3-(Cyclopentyloxy)-4-methoxyphenyl)-2-hydrazinyl-6-oxo-1,6-dihydropyrimidine-5-carbonitrile (12)

A mixture of compound **10** (0.343 g, 1 mmol) and hydrazine hydrate (0.92 g, 3 mmol) were refluxed in ethanol. Upon completion of the reaction as judged by TLC, a pale white solid was formed, filtered, and recrystallized from ethanol. Yield 95%. Pale white solid. Mp: 200°C. IR (KBr, cm^{-1}) 3445 (NH_2), 3327 (NH), 2958 (aliph. CH), 2188 (CN), 1657 (CN). ^{1}H NMR (500 MHz, DMSO-d_6, δ, ppm) δ 11.22 (s, 2H), 7.49 (dd, J = 8.6, 2.1 Hz, 1H), 7.46 (d, J = 2.1 Hz, 1H), 7.09 (d, J = 8.6 Hz, 1H), 4.79 (m, 1H), 3.82 (s, 3H), 2.42 (t, J = 7.2 Hz, 2H), 2.16–1.51 (m, 8H). Elemental analysis for $C_{17}H_{19}N_5O_3$, calcd.: C, 59.81; H, 5.61; N, 20.52. Found: C, 59.83; H, 5.63; N, 20.52.

4.1.3 | General procedure for the preparation of compounds 13a–g

A mixture of compound **12** (0.341 g, 1 mmol) and appropriate aromatic aldehydes (1 mmol) were refluxed in ethanol for 12 h, till completion of the reaction as judged by TLC. The precipitates were filtered and recrystallized from ethanol.

(*E*)-4-(3-(Cyclopentyloxy)-4-methoxyphenyl)-2-(2-(furan-2-ylmethylene)hydrazinyl)-6-oxo-1,6-dihydropyrimidine-5-carbonitrile (13a)

Yield 33%. White solid. Mp: 125–126°C. ^{1}H NMR (500 MHz, DMSO-d_6, δ, ppm) δ 11.8 (s,1H), 12.8 (s, 1H), 8.1 (s, 1H),7.87 (d, J = 1.2 Hz, 1H), 7.52 (dd, J = 8.5, 2.0 Hz, 1H), 7.48 (d, J = 2.0 Hz, 1H), 7.25 (d, J = 3.0 Hz, 1H), 7.11 (d, J = 8.6 Hz, 1H), 6.67 (dd, J = 3.4, 1.7 Hz, 1H), 4.80 (m, 1H), 3.83 (s, 3H), 1.98–1.53 (m, 8H). ^{13}C NMR (125 MHz, DMSO-d_6, δ, ppm) δ 170.55, 152.93, 150.63, 147.16, 146.38, 146.15, 122.72, 115.16, 113.91, 113.25, 112.15, 80.50, 56.36, 33.03, 24.30. Elemental analysis

for $C_{22}H_{21}N_5O_4$, calcd.: C, 63.00; H, 5.05; N, 16.70. Found: C, 63.02; H, 5.06; N, 16.71.

(*E*)-2-(2-Benzylidenehydrazinyl)-4-(3-(cyclopentyloxy)-4-methoxyphenyl)-6-oxo-1,6-dihydropyrimidine-5-carbonitrile (13b)

Yield 49%. White solid. Mp: 265°C. ^{1}H NMR (500 MHz, $CDCl_3$, δ, ppm) δ 11.5–12.5 (s, 2H), 8.5 (s, 1H), 8.23 (d, *J* = 7.8 Hz, 1H), 8.01 (d, *J* = 7.3 Hz, 2H), 7.2–7.9 (m, 5H), 4.80 (m, 1H), 3.83 (s, 3H), 1.98–1.53 (m, 8H). ^{13}C NMR (125 MHz, DMSO-d_6, δ, ppm) δ 170.07, 162.45, 153.64, 152.73, 147.39, 146.82, 134.22, 130.88, 129.05, 128.57, 122.44, 118.09, 115.02, 111.96, 85.94, 80.33, 56.17, 32.86, 24.12. Elemental analysis for $C_{24}H_{23}N_5O_3$, calcd.: C, 67.12; H, 5.40; N, 16.31. Found: C, 67.13; H, 5.42; N, 16.31.

(*E*)-4-(3-(Cyclopentyloxy)-4-methoxyphenyl)-2-(2-(4-hydroxybenzylidene)hydrazinyl)-6-oxo-1,6-dihydropyrimidine-5-carbonitrile (13c)

The product was purified by column chromatography (pet. ether/ethyl acetate 3:1). Yield 25%. Yellow solid. Mp: 171–172°C. IR (KBr, cm^{-1}) 3445 (NH), 3424 (OH), 2924 (aliph. CH), 2215 (CN), and 1661 (CO). ^{1}H NMR (500 MHz, DMSO-d_6, δ, ppm) δ 12.27 (s, 1H), 12.14 (s, 1H), 9.99 (s, 1H), 8.08 (s, 1H), 7.84 (d, *J* = 8.6 Hz, 2H), 7.52 (dd, *J* = 8.4, 2.1 Hz, 1H), 7.48 (d, *J* = 2.1 Hz, 1H), 7.10 (d, *J* = 8.6 Hz, 1H), 6.80 (d, *J* = 8.7 Hz, 2H), 4.79 (m, 1H), 3.82 (s, 1H), 2.03–1.52 (m, 8H). Elemental analysis for $C_{24}H_{23}N_5O_4$, calcd.: C, 64.71; H, 5.20; N, 15.72. Found: C, 64.72; H, 5.23; N, 15.72.

(*E*)-4-(3-(Cyclopentyloxy)-4-methoxyphenyl)-2-(2-(3-nitrobenzylidene)hydrazinyl)-6-oxo-1,6-dihydropyrimidine-5-carbonitrile (13d)

Yield 97%. Bright yellow. Mp: 255–256°C. IR (KBr, cm^{-1}) 3447 (NH), 2963 (aliph. CH), 2213 (CN), 1548–1343 (NO). ^{1}H NMR (500 MHz, $CDCl_3$, δ, ppm) δ 12.3 (s, 2H), 8.90 (s, 2H), 8.43 (d, *J* = 7.7 Hz, 1H), 8.3 (s, 1H), 8.25 (d, *J* = 8.1 Hz, 1H), 7.72 (t, *J* = 8.0 Hz, 1H), 7.55 (d4, *J* = 8.4, 2.1 Hz, 1H), 7.51 (d, *J* = 2.1 Hz, 1H), 7.12 (d, *J* = 8.6 Hz, 1H), 4.80 (m, 1H), 3.85 (s, 3H), 1.99–1.43 (m, 8H). ^{13}C NMR (125 MHz, DMSO-d_6, δ, ppm) δ 170.06, 162.51, 153.31, 152.63, 152.25, 148.32, 146.80, 130.06, 128.84, 122.37, 121.48, 118.36, 115.02, 111.95, 84.87, 80.33, 56.17, 32.88, 24.14. Elemental analysis for $C_{24}H_{22}N_6O_5$, calcd.: C, 60.75; H, 4.67; N, 17.71. Found: C, 60.77; H, 4.67; N, 17.73.

(*E*)-4-(3-(Cyclopentyloxy)-4-methoxyphenyl)-2-(2-(2-methoxybenzylidene)hydrazinyl)-6-oxo-1,6-dihydropyrimidine-5-carbonitrile (13e)

It was purified with column chromatography (pet. ether/ethyl acetate 3:1). Yield 25%. Yellow solid. Mp: 250–251°C. ^{1}H NMR (500 MHz, $CDCl_3$, δ, ppm) δ 8.43 (s, 1H), 7.84 (d, *J* = 7.6 Hz, 1H), 7.59 (dd, *J* = 8.3, 2.1 Hz, 1H), 7.44 (d, *J* = 2.1 Hz, 1H), 7.38 (t, *J* = 7.9 Hz, 1H), 6.98 (t, *J* = 7.5 Hz, 1H), 6.88 (d, *J* = 8.5 Hz, 1H), 6.85 (d, *J* = 8.4 Hz, 1H), 4.86–4.71 (m, 1H), 3.82 (s, 3H), 3.81 (s, 3H), 1.98–1.53 (m, 8H). Elemental analysis for $C_{25}H_{25}N_5O_4$, calcd.: C, 65.35; H, 5.48; N, 15.24. Found: C, 65.39; H, 5.49; N, 15.24.

(*E*)-4-(3-(Cyclopentyloxy)-4-methoxyphenyl)-2-(2-(4-(dimethylamino)benzylidene)hydrazinyl)-6-oxo-1,6-dihydropyrimidine-5-carbonitrile (13f)

Yield 60%. Yellow solid. Mp: 259–260°C. ^{1}H NMR (500 MHz, DMSO-d_6, δ, ppm) δ11.5–12.5 (s, 1H), 8.05 (s, 1H), 7.79 (d, *J* = 8.7 Hz, 2H), 7.51 (dd, *J* = 8.6, 2.1 Hz, 1H), 7.5 (d, *J* = 2.1 Hz, 1H), 7.09 (d, *J* = 8.6 Hz, 1H), 6.71 (d, *J* = 9.0 Hz, 2H), 4.79 (m, 1H), 3.82 (s, 3H), 2.98 (s, 6H), 1.98–1.53 (m, 8H). Elemental analysis for $C_{26}H_{28}N_6O_3$, calcd.: C, 66.09; H, 5.97; N, 17.78. Found: C, 66.11; H, 5.98; N, 17.76.

(*E*)-4-(3-(Cyclopentyloxy)-4-methoxyphenyl)-2-(2-(3-hydroxy-4-methoxybenzylidene)hydrazinyl)-6-oxo-1,6-dihydropyrimidine-5-carbonitrile (13g)

Yield 58%. White solid. Mp: 292–293°C. ^{1}H NMR (500 MHz, DMSO-d_6, δ, ppm) δ 12.21 (s, 2H), 9.04 (s, 1H), 8.05 (s, 1H), 7.57 (s, 1H), 7.53 (dd, *J* = 8.4,2.0 Hz, 1H), 7.49 (d, 2.0 Hz, 1H), 7.28 (d, *J* = 8.4 Hz, 1H), 7.11 (d, *J* = 8.6 Hz, 1H), 6.97 (d, *J* = 8.4 Hz, 1H), 4.80 (m, 1H), 3.83 (s, 6H), 1.98–1.53 (m, 8H). ^{13}C NMR (125 MHz, DMSO-d_6, δ, ppm) δ 170.16, 152.67, 150.53, 147.75, 147.09, 146.81, 128.73, 127.14, 122.38, 121.61, 118.19, 115.01, 114.58, 111.94, 85.49, 80.32, 56.17, 32.86, 24.12. Elemental analysis for $C_{25}H_{25}N_5O_5$, calcd.: C, 63.15; H, 5.30; N, 14.73. Found: C, 63.17; H, 5.31; N, 14.74.

4-(3-(Cyclopentyloxy)-4-methoxyphenyl)-2-((*E*)-2-((2*E*,4*E*)-4-methylhexa-2,4-dienylidene)hydrazinyl)-6-oxo-1,6-dihydropyrimidine-5-carbonitrile (13h)

Yield 45%. Bright yellow solid. Mp: 175–176°C. ^{1}H NMR (500 MHz, DMSO-d_6, δ, ppm) δ 11.5–12.5 (s, 2H), 8.02 (d, *J* = 9.1 Hz, 1H), 7.58 (dd, *J* = 7.4 Hz, 2H), 7.52 (dd, *J* = 8.5, 2.1 Hz, 1H), 7.48 (d, *J* = 2.1 Hz, 1H), 7.42 (t, *J* = 7.5 Hz, 2H), 7.35 (t, *J* = 7.3 Hz, 1H), 7.15 (d, *J* = 16.2 Hz, 1H), 7.11 (d, *J* = 8.6 Hz, 1H), 6.99 (dd, *J* = 16.3, 9.2 Hz, 1H), 4.80 (m, 1H), 3.85 (s, 3H), 1.99–1.43 (m, 8H). ^{13}C NMR (125 MHz, DMSO-d_6, δ, ppm) δ 171.33, 169.99, 153.95, 153.25, 149.49, 149.33, 147.33, 140.73, 136.75, 130.00, 129.61, 128.08, 125.69, 122.95, 118.53, 115.52, 112.48, 80.84, 56.69, 33.36, 24.62. Elemental analysis for $C_{26}H_{25}N_5O_3$, calcd.: C, 68.56; H, 5.53; N, 15.37. Found: C, 68.58; H, 5.54; N, 15.37.

(*Z*)-2-(3-(Cyclopentyloxy)-4-methoxybenzylidene)hydrazinecarbothioamide (14)

A mixture of of compound **9** (0.220, 1 mmol) and thiosemicarbazide (0.075g, 1 mmol) was refluxed in ethanol overnight. Upon completion of the reaction as judged by TLC, the cold reaction mixture was poured into crushed ice and the separated solid was filtered off and was recrystallized from ethanol. Yield 60%. Pale yellow solid. Mp:165–166°C. IR (KBr, cm$^{-1)}$ 3413 (NH), 3294–3163 (NH_2), 2962 (aliph. CH). ^{1}H NMR (500 MHz, DMSO-d_6, δ, ppm) δ 11.29 (s, 1H), 8.14 (s, 1H), 7.94 (s, 1H), 7.45 (d, *J* = 2.1 Hz, 1H), 7.12 (dd, *J* = 8.2, 2.0 Hz, 1H), 6.94 (d, *J* = 8.4 Hz, 1H), 4.94 (m, 1H), 4.49 (s, 2H), 3.76 (s, 3H), 1.93–1.51 (m, 8H). Elemental analysis for $C_{14}H_{19}N_3O_2S$, calcd.: C, 57.32; H, 6.53; N, 14.32. Found: C, 57.31; H, 6.55; N, 14.34.

(*Z*)-2-(2-(3-(Cyclopentyloxy)-4-methoxybenzylidene)hydrazinyl)-thiazol-4(5*H*)-one (15)

A mixture of compound **14** (0.293 g, 1 mmol), ethyl chloroacetate (0.122 g, 1 mmol) and sodium acetate (0.082 g, 1 mmol) was refluxed in acetic acid for 10 h. Upon completion of the reaction as judged by TLC, the reaction mixture was allowed to cool then it was poured into crushed ice. The formed solid was filtered off, washed with water, dried and recrystallized from aqueous ethanol to give the pure product. Yield 48%. Brown solid. Mp: 220–221°C. ^{1}H NMR (500 MHz, DMSO-d_6, δ, ppm) δ 11.89 (s, 1H), 8.28 (s, 1H), 7.36 (d, *J* = 2.0 Hz, 1H), 7.25 (dd, *J* = 8.4, 2.0 Hz, 1H), 7.02 (d, *J* = 8.4 Hz, 1H), 4.90–4.69 (m, 1H), 3.84 (s, 2H), 3.79 (s, 3H), 1.99–1.50 (m, 8H). ^{13}C NMR (125 MHz, DMSO-d_6, δ, ppm) δ 176.00, 155.43, 152.20, 147.59, 127.66, 122.24, 112.54, 112.36, 80.09, 56.08, 33.79, 32.84, 24.23. Elemental analysis for $C_{16}H_{19}N_3O_3S$, calcd.: C, 57.64; H, 5.74; N, 12.60. Found: C, 57.66; H, 5.75; N, 12.61.

(*Z*)-2-(2-(2-(3-(Cyclopentyloxy)-4-methoxybenzylidene)-hydrazinyl)-4-oxo-4,5-dihydrothiazol-5-yl)acetic acid (16)

A mixture of compound **14** (0.293 g, 1 mmol) and maleic anhydride (0.89 g, 1 mmol) were refluxed in toluene/DMF 25:1 for 12 h. After completion of the reaction as judged by TLC, the reaction mixture was allowed to cool then poured into crushed ice. The formed solid was filtered off, washed with water, and recrystallized from aqueous ethanol to give the pure product. Yield 40%. White solid. Mp: 236–237°C. IR (KBr, cm^{-1}) 3425 (NH), 3423 (OH), 2960 (aliph. CH), 1715 (CO), 1642 (CO). ^{1}H NMR (500 MHz, DMSO-d_6, δ, ppm) δ 11.94 (s, 1H), 8.29 (s, 1H), 7.34 (d, *J* = 2.0 Hz, 1H), 7.26 (dd, *J* = 8.3, 2.1 Hz, 1H), 7.01 (d, *J* = 8.4 Hz, 1H), 4.89–4.68 (m, 1H), 4.33 (dd, *J* = 8.6, 3.9 Hz, 1H), 3.79 (s, 3H), 3.00 (dd, *J* = 17.6, 3.8 Hz, 1H), 2.89 (dd, *J* = 17.7, 8.6 Hz, 1H), 1.96–1.49 (m, 8H). ^{3}C NMR (125 MHz, δ, ppm) δ 175.98, 172.39, 156.68, 152.57, 147.75, 127.54, 122.59, 112.55, 112.55, 80.28, 56.26, 44.18, 37.26, 33.97, 32.99, 24.37. Elemental analysis for $C_{18}H_{21}N_3O_5S$, calcd.: C, 55.23; H, 5.41; N, 10.73. Found: C, 55.25; H, 5.42; N, 10.71.

(*Z*)-Methyl-2-(2-(2-(3-(cyclopentyloxy)-4-methoxybenzylidene)-hydrazinyl)-4-oxo-4,5-dihydrothiazol-5-yl)acetate (17)

A mixture of compound **14** (0.293 g, 1 mmol) and DMAD (0.142 g, 1 mmol) was refluxed in ethanol. After 1 h, the formed solid was allowed to cool and then filtered off and recrystallized from ethanol. Yield 42%. Yellow solid. Mp: 260–261°C. IR (KBr, cm^{-1}) 3424 (NH), 2954 (aliph. CH), 1727 (CO), 1702 (CO), 1644 (CN). ^{1}H NMR (500 MHz, DMSO-d_6, δ, ppm) δ 8.44 (s, 1H), 7.40 (d, *J* = 2.0 Hz, 1H), 7.37 (dd, *J* = 8.3, 2.0 Hz, 1H), 7.07 (d, *J* = 8.4 Hz, 1H), 6.67 (s, 1H), 4.88–4.77 (m, 1H), 3.81 (s, 3H), 3.79 (s, 3H), 2.00–1.56 (m, 8H). ^{13}C NMR (125 MHz, MHz, DMSO-d_6, δ, ppm) δ 169.07, 151.38, 149.87, 147.73, 142.03, 132.05, 128.04, 127.61, 120.98, 120.73, 112.51, 111.54, 104.85, 80.08, 56.08, 32.88, 24.27. Elemental analysis for $C_{19}H_{23}N_3O_5S$, calcd.: C, 56.28; H, 5.72; N, 10.36. Found: C, 56.29; H, 5.73; N, 10.37.

(*Z*)-Ethyl-2-(2-(3-(Cyclopentyloxy)-4-methoxybenzylidene)-hydrazinyl)-4,5-dihydrothiazole-5-carboxylate (18)

A mixture of compound **14** (0.293 g, 1 mmol) and ethyl 4-chloroacetoacetate (0.164 g, 1 mmol) was refluxed in ethanol. After completion of the reaction as judged by TLC the reaction mixture was allowed to cool then poured into crushed ice. The formed solid was filtered off, washed with water, dried and recrystallized from aqueous ethanol to give the pure product. Buff solid. Mp: 140–141°C. ^{1}H NMR (500 MHz, DMSO-d_6, δ, ppm) δ 11.87 (s, 1H), 7.88 (s, 1H), 7.2 (d, *J* = 2.0 Hz, 1H), 7.11 (dd, *J* = 8.2,2.0 Hz, 1H), 6.97 (d, *J* = 8.4 Hz, 1H), 6.61 (s, 1H), 4.85–4.74 (m, 1H), 4.07 (q, *J* = 7.0 Hz, 2H), 3.76 (s, 3H), 3.57 (s, 2H), 2.05–1.40 (m, 8H), 1.18 (t, *J* = 7.1 Hz, 3H). ^{13}C NMR (125 MHz, DMSO-d_6, δ, ppm) δ 170.65, 168.85, 151.58, 147.87, 142.49, 127.76, 120.92, 112.67, 111.82, 106.13, 80.24, 60.99, 56.25, 37.42, 32.03, 32.87, 24.42, 14.79. Elemental analysis for $C_{20}H_{25}N_3O_4S$, calcd.: C, 59.53; H, 6.25; N, 10.41. Found: C, 59.55; H, 6.27; N, 10.42.

4.1.4 | General procedure for the preparation of compounds 19a–c

A mixture of compound **14** (0.293 g, 1 mmol) and an appropriate phenacyl bromide (1 mmol) was refluxed in ethanol till completion of the reaction as judged by TLC. The reaction mixture was allowed to cool then the solid was filtered off and recrystallized from ethanol.

(*Z*)-2-(2-(3-(Cyclopentyloxy)-4-methoxybenzylidene)hydrazinyl)-5-phenylthiazole (19a)

Yield 49%. Off-white solid. Mp: 170–171°C. ^{1}H NMR (500 MHz, DMSO-d_6, δ, ppm) δ 12.05 (s, 1H), 7.96 (s, 1H), 7.85 (d, *J* = 7.1 Hz, 2H), 7.41 (t, *J* = 7.7 Hz, 2H), 7.35–7.22 (m, 2H), 7.27 (d, *J* = 1.9 Hz, 1H), 7.15 (dd, *J* = 8.3, 1.8 Hz, 1H), 7.00 (d, *J* = 8.4 Hz, 1H), 4.83–4.70 (m, 1H), 3.77 (s, 3H), 1.93–1.51 (m, 8H). ^{13}C NMR (126 MHz, DMSO-d_6, δ, ppm) δ 169.12, 151.64, 147.90, 142.72, 129.32, 129.00, 128.52, 127.70, 126.26, 121.01, 112.68, 112.68, 111.80, 104.22, 80.26, 56.26, 33.04, 24.42. Elemental analysis for $C_{22}H_{23}N_3O_2S$, calcd.: C, 67.15; H, 5.89; N, 10.68. Found: C, 67.17; H, 5.90; N, 10.70.

(*Z*)-5-(4-Bromophenyl)-2-(2-(3-(cyclopentyloxy)-4-methoxy-benzylidene)hydrazinyl)thiazole (19b)

Yield 60%. Buff solid. Mp: 210°C. IR (KBr, cm^{-1}) 3336 (NH), 2959 (aliph. CH), 1625 (C═N). ^{1}H NMR (500 MHz, DMSO-d_6, δ, ppm) δ 12.05 (s, 1H), 7.94 (s, 1H), 7.80 (d, *J* = 7.0 Hz, 2H), 7.59 (d, *J* = 10.9 Hz, 2H), 7.38 (s, 1H), 7.26 (d, *J* = 2.0 Hz, 1H), 7.14 (dd, *J* = 8.3, 2.0 Hz, 1H), 6.99 (d, *J* = 8.3 Hz, 1H), 4.83–4.70 (m, 1H), 3.77 (s, 3H), 1.93–1.51 (m, 8H). ^{13}C NMR (125 MHz, DMSO-d_6, δ, ppm) δ 169.41, 151.72, 150.73, 148.06, 142.36, 137.79, 132.38, 128.37, 127.95, 121.31, 121.06, 112.84, 111.87, 105.18, 80.41, 56.42, 33.22, 24.60. Elemental analysis for $C_{22}H_{22}BrN_3O_2S$, calcd.: C, 55.94; H, 4.69; N, 8.90. Found: C, 55.96; H, 4.68; N, 8.92.

(*Z*)-5-(4-Chlorophenyl)-2-(2-(3-(cyclopentyloxy)-4-methoxy-benzylidene)hydrazinyl)thiazole (19c)

Yield 48%. Buff solid. Mp: 190–191°C. ^{1}H NMR (500 MHz, DMSO-d_6, δ, ppm) δ 12.05 (s, 1H), 7.94 (s, 1H), 7.80 (d, *J* = 7.0 Hz, 2H), 7.59 (d, *J* = 10.9 Hz, 2H), 7.38 (s, 1H), 7.26 (d, *J* = 2.0 Hz, 1H), 7.14 (dd, *J* = 8.3, 2.0 Hz, 1H), 6.99 (d, *J* = 8.3 Hz, 1H), 4.83–4.70 (m, 1H), 3.77 (s, 3H), 1.93–1.51 (m, 8H). ^{13}C NMR (126 MHz, DMSO-d_6, δ, ppm) δ 168.71, 151.04, 147.38, 141.73, 134.07, 131.69, 127.68, 127.26,

120.64, 120.38, 112.16, 111.22, 104.49, 79.73, 55.73, 32.53, 23.91. Elemental analysis for $C_{22}H_{22}ClN_3O_2S$, calcd.: C, 61.75; H, 5.18; N, 9.82. Found: C, 61.75; H, 5.19; N, 9.84.

2-(3-(Cyclopentyloxy)-4-methoxybenzylidene)malononitrile (20)

A mixture of compound **8** (0.220 g, 1 mmol) and malononitrile (0.24 g, 4 mmol) were refluxed in ethanol for 12 h. After completion of the reaction as judged by TLC, the reaction mixture was allowed to cool and the solvent was allowed to evaporate slowly. Yellow crystals were formed, filtered off, dried and recrystallized from ethanol to give the pure product. Yield 66%. Yellow crystals. Mp: 132–133°C. IR (KBr, cm^{-1}) 3023, 3965 (aliph. CH), 2221 (CN). ^{1}H NMR (500 MHz, DMSO-d_6, δ, ppm) δ 8.36 (s, 1H), 7.66 (d, J = 2.1 Hz, 1H), 7.55 (dd, J = 8.5, 2.1 Hz, 1H), 7.20 (d, J = 8.6 Hz, 1H), 4.74 (m, 1H), 3.88 (s, 3H), 2.06–1.48 (m, 8H). ^{13}C NMR (125 MHz, DMSO-d_6, δ, ppm) δ 160.69, 155.17, 144.13, 124.09, 127.72, 114.89, 114.09, 113.54, 112.20, 79.87, 76.42, 56.06, 32.22, 23.71. Elemental analysis for $C_{16}H_{16}N_2O_2$, calcd.: C, 71.62; H, 6.01; N, 10.44. Found: C, 71.64; H, 6.02; N, 10.45.

4.1.5 | General procedure for the preparation of compounds 21 and 22

A mixture of compound **20** (0.268 g, 1 mmol) and appropriate β-dicarbonyl compound (1 mmol) were stirred for 2 h in dry ether. The product was obtained by evaporating the solvent. It was purified by column chromatography (petroluem ether/ethyl acetate 3:1).

5-Acetyl-2-amino-4-(3-(cyclopentyloxy)-4-methoxyphenyl)-4*H*-pyran-3-carbonitrile (21)

Yield 15%. Orange solid. Mp: 122–123°C. ^{1}H NMR (500 MHz, DMSO-d_6, δ, ppm) δ 8.09 (s, 1H), 7.88–7.55 (m, 3H), 7.49 (dd, J = 8.5, 2.0 Hz, 1H), 7.14 (d, J = 8.5 Hz, 1H), 4.77 (m, 1H), 3.84 (s, 3H), 3.72 (s, 1H), 2.64–2.39 (m, 6H), 1.99–1.85 (m, 2H), 1.80–1.66 (m, 5H), 1.62–1.52 (m, 3H). Elemental analysis for $C_{20}H_{22}N_2O_4$, calcd.: C, 67.78; H, 6.26; N, 7.90. Found: C, 67.80; H, 6.27; N, 7.91.

Ethyl 6-amino-5-cyano-4-(3-(cyclopentyloxy)-4-methoxyphenyl)-2-methyl-4*H*-pyran-3-carboxylate (22)

Yield 56%. Orange solid. Mp: 91–92°C. IR (KBr, cm^{-1}) 3421, 3329 (NH_2), 2957 (aliph. CH), 2197 (CN), 1712 (CO). ^{1}H NMR (500 MHz, DMSO-d_6, δ, ppm) δ 6.91–6.85 (m, 3H), 6.67 (d, J = 2.1 Hz, 1H), 6.63 (dd, J = 8.2, 2.0 Hz, 1H), 4.70 (m, 1H), 4.23 (s, 1H), 4.04–3.93 (q, 7.2 Hz, 2H), 3.71 (s, 3H), 2.29 (s, 3H), 1.92–1.49 (m, 8H), 1.06 (t, J = 7.1 Hz, 3H). ^{13}C NMR (126 MHz, DMSO-d_6, δ, ppm) δ 166.10, 158.92, 156.52, 149.00, 147.08, 137.73, 120.32, 119.52, 114.69, 112.82, 108.00, 79.99, 60.66, 57.88, 56.02, 38.68, 32.71, 24.04, 18.56, 14.31. Elemental analysis for $C_{22}H_{26}N_2O_5$, calcd.: C, 66.32; H, 6.58; N, 7.03. Found: C, 66.34; H, 6.59; N, 7.04.

4.1.6 | General procedure for the preparation of compounds 23 and 24

A mixture of compound **20** (0.286 g, 1 mmol) and appropriate phenolic compound (1 mmol) were refluxed in toluene in presence of few drops of piperidine. After 10 h the reaction was completed as judged by TLC. The reaction mixture was allowed to cool, then poured into crushed ice. The formed solid was filtered off, dried and recrystallized from ethanol.

2-Amino-4-(3-(cyclopentyloxy)-4-methoxyphenyl)-7-hydroxy-4*H*-chromene-3-carbonitrile (23)

Yield 70%. White solid. Mp: 175–176°C. IR (KBr, cm^{-1}) 3437 (NH_2), 3341 (OH), 2960 (aliph. CH), 2188 (CN). ^{1}H NMR (500 MHz, DMSO-d_6, δ, ppm) δ 9.66 (s, 1H), 6.86 (d, J = 8.2 Hz, 1H), 6.84–6.79 (m, 3H), 6.72 (d, J = 2.0 Hz, 1H), 6.63 (dd, J = 8.2, 2.0 Hz, 1H), 6.48 (dd, J = 8.4, 2.5 Hz, 1H), 6.38 (d, J = 2.3 Hz. 1H), 4.68 (m, 1H), 4.54 (s, 1H), 3.69 (s, 3H), 1.97–1.42 (m, 8H). ^{13}C NMR (125 MHz, DMSO-d_6, δ, ppm) δ 160.17, 156.93, 148.7, 148.30, 146.79, 138.76, 129.84, 120.72, 119.25, 114.24, 114.04, 112.34, 112.27, 102.05, 79.40, 56.42, 55.53, 39.83, 32.18, 23.53. Elemental analysis for $C_{22}H_{22}N_2O_4$, calcd.: C, 69.83; H, 5.86; N, 7.40. Found: C, 69.84; H, 5.87; N, 7.42.

2-Amino-4-(3-(cyclopentyloxy)-4-methoxyphenyl)-4*H*-benzo[h]-chromene-3-carbonitrile (24)

Yield 50%. White solid. 170–171°C. ^{1}H NMR (500 MHz, DMSO-d_6, δ, ppm) δ 8.22 (d, J = 8.1 Hz, 1H), 7.88 (d, J = 8.1 Hz, 1H), 7.64–7.45 (m, 3H), 7.16–7.03 (m, 3H), 6.86 (d, J = 8.4 Hz, 1H), 6.84 (d, J = 2.1 Hz, 1H), 6.69 (dd, J = 8.3, 2.0 Hz, 1H), 4.68 (m, 1H), 4.54 (s, 1H), 3.69 (s, 3H), 1.97–1.42 (m, 8H). ^{13}C NMR (125 MHz, DMSO-d_6, δ, ppm) δ 160.07, 148.50, 146.84, 142.56, 138.06, 132.62, 128.90, 128.21, 127.68, 126.25, 125.32, 123.74, 122.72, 120.61, 119.65, 118.20, 114.50, 112.44, 79.42, 56.35, 55.52, 40.27, 32.15, 23.51. Elemental analysis for $C_{26}H_{24}N_2O_3$, calcd.: C, 75.71; H, 5.86; N, 6.79. Found: C, 75.72; H, 5.88; N, 6.80.

2-Amino-4-(3-(cyclopentyloxy)-4-methoxyphenyl)-6,6-dimethyl-8-oxo-5,6,7,8-tetrahydro-4*H*-chromene-3-carbonitrile (25)

In a typical procedure, equimolar amounts of compound **9** (0.220 g), malononitrile (0.066 g) and dimedone (0.140 g) were mixed with tetrabutylammonium bromide (10 mol%) in 15 mL 90% ethanol and refluxed with stirring for 12 h. After the completion of the reaction, the mixture was cooled to room temperature and poured into crushed ice. The solid was filtered off, dried, and recrystallized from ethanol to give the pure product. Yield 54%. White solid. Mp: 158–159°C; IR (KBr, cm^{-1}) 3401 (NH_2), 2962 (aliph. CH), 2194 (CN), 1671 (CO). ^{1}H NMR (500 MHz, DMSO-d_6, δ, ppm) δ 6.77 (s, 1H), 6.76 (d, J = 8.2 Hz, 1H), 6.71 (dd, J = 8.3, 2.0 Hz, 1H), 4.75 (m, 1H), 4.52 (s, 2H), 4.33 (s, 1H), 3.78 (s, 3H), 2.43 (s, 2H), 2.22 (s, 2H), 1.92–1.49 (m, 8H), 1.10 (s, 3H), 1.03 (s, 3H). Elemental analysis for $C_{24}H_{28}N_2O_4$, calcd.: C, 70.57; H, 6.91; N, 6.86. Found: C, 70.59; H, 6.93; N, 6.87.

4.2 | Biological assays

4.2.1 | Enzyme assay protocol

The inhibition of PDE4 enzyme was measured using PDE4B (cAMP-specific 3′,5′-cyclicphosphodiesterase 4B) ELISA Kit (MBS761396)

according to manufacturer's recommendations. In brief, FAM-cyclic-3′,5′-AMP (200 nM) was added to each well. The PDE assay buffer was added after which the inhibitor solution was added. The reaction was initiated by adding PDE4B2 to the well, then they were incubated at room temperature for 1 h. Diluted binding agent was added to each microwell and then incubated at room temperature for 1 h with slow shaking. The fluorescent polarization of the sample was read in a microtiter-plate reader equipped for the measurement of fluorescence polarization, capable of excitation at wavelengths ranging from 475 to 495 nm and detection of emitted light ranging from 518 to 538 nm.

4.2.2 | Analysis of cellular apoptosis

Cells were plated in a density of $1.2–1.8 \times 10^4$ cells/well in a volume of 100 µL complete growth medium + 100 µL of the tested compound per well in a 96-well plate. Apoptosis was induced. $1–5 \times 10^5$ cells were collected by centrifugation. Cells were suspended in 500 µL of binding buffer. A total of 5 µL of Annexin V-FITC and 5 µL of propidium iodide was added. Then they were incubated at room temperature for 5 min in the dark. Annexin V-FITC binding was analyzed by flow cytometry using FITC signal detector and PI staining by the phycoerythrin emission signal detector.

4.2.3 | Flow cytometric analysis of cell cycle distribution

For flow cytometric analysis of DNA content, 5×10^5 EC-109 cells in exponential growth were treated with the test compounds for 24 h. The cells were collected and centrifuged in tubes containing 4.5 mL of 70% ethanol, on ice. The cell pellets were suspended in 1 mL of PI staining solution, kept in the dark at room temperature for 30 min, or at 37°C for 10 min. Samples were transferred to the flow cytometer and measure cell fluorescence. Maximum excitation of PI bound to DNA is at 536 nm, and emission is at 617 nm. Blue (488 nm) or green light lines of lasers are optimal for excitation of PI fluorescence. Emission was measured using the long-pass 600- or 610-nm filter for data acquisition, interpretation.

4.2.4 | Enzyme-linked immunosorbent assay of caspase-3 and -9

The Invitrogen Caspase-3 (active) Human ELISA kit was used to detect and quantify the level of human active caspase-3 protein according to manufacturers' instructions. Briefly, cells were grown in RPMI 1640 containing 10% fetal bovine serum at 37°C, stimulated with the compounds to be tested for caspase-3, and lysed with cell extraction buffer. Wells were incubated for 2 h at room temperature then washed four times. A total of 100 µL of Caspase-3 (Active) detection antibody solution was added to each well and incubated for 1 h at room temperature. The wells were washed and 100 µL Anti-Rabbit IgG HRP working solution was added to each well and incubated for 30 min at room temperature. After washing, 100 µL of stabilized chromogen was added to each well. The liquid in the wells began to turn blue. After adding the stop solution, the absorbance of each well was measured at 450 nm.

The same procedure was used for determination of caspase-9 using The Invitrogen Caspase-9 (active) Human ELISA kit.

ACKNOWLEDGMENTS

This work was supported by Research Unit, Mansoura University (project by Dr. Magda A.-A. El-Sayed). We are grateful to Holding Company for biological products and vaccines (VACSERA), Giza, Egypt, for performing all of the biological analysis.

CONFLICT OF INTEREST

The authors have declared no conflict of interest.

ORCID


Magda A.-A. El-Sayed http://orcid.org/0000-0001-9599-9248

REFERENCES

[1] M. D. Houslay, P. Schafer, K. Y. Zhang, *Drug Discov. Today* **2005**, *10*, 1503.
[2] S. L. C. Jin, L. Lan, M. Zoudilova, M. Conti, *J. Immunol.* **2005**, *175*, 1523.
[3] A. Robichaud, P. B. Stamatiou, S. L. Jin, N. Lachance, D. MacDonald, F. Laliberté, S. Liu, Z. Huang, M. Conti, C. C. Chan, *Eur. J. Clin. Invest.* **2002**, *110*, 1045.
[4] M. Kranz, M. Wall, B. Evans, A. Miah, S. Ballantine, C. Delves, B. Dombroski, J. Gross, J. Schneck, J. P. Villa, *Bioorg. Med. Chem.* **2009**, *17*, 5336.
[5] D. R. Gorja, S. Mukherjee, C. L. Meda, G. S. Deora, K. L. Kumar, A. Jain, G. H. Chaudhari, K. S. Chennubhotla, R. K. Banote, P. Kulkarni, K. V. Parsa, *Org. Biomol. Chem.* **2013**, *11*, 2075.
[6] K. Naganuma, A. Omura, N. Maekawara, M. Saitoh, N. Ohkawa, T. Kubota, H. Nagumo, T. Kodama, M. Takemura, Y. Ohtsuka, J. Nakamura, *Bioorg. Med. Chem. Lett.* **2009**, *19*, 3174.
[7] A. F. Donnell, P. J. Dollings, J. A. Butera, A. J. Dietrich, K. K. Lipinski, A. Ghavami, W. D. Hirst, *Bioorg. Med. Chem. Lett.* **2010**, *2*, 2163.
[8] S. Contreras, J. Milara, E. Morcillo, J. Cortijo, *Curr. Pharm. Des.* **2017**, *23*, 2073.
[9] A. Kodimuthali, S. S. L. Jabaris, M. Pal, *J. Med. Chem.* **2008**, *51*, 5471.
[10] N. Parikh, A. K. Chakraborti, *Curr. Med. Chem.* **2016**, *23*, 129.
[11] R. Savai, S. S. Pullamsetti, G. A. Banat, N. Weissmann, H. A. Ghofrani, F. Grimminger, R. T. Schermuly, *Expert Opin. Investig. Drugs* **2010**, *19*, 117.
[12] P. V. Babu, S. Mukherjee, G. S. Deora, K. S. Chennubhotla, R. Medisetti, S. Yellanki, *Org. Biomol. Chem.* **2013**, *11*, 6680.
[13] J. Mareddy, N. Suresh, C. G. Kumar, R. Kapavarapu, A. Jayasree, S. Pa, *Bioorg. Med. Chem. Lett.* **2017**, *27*, 518.
[14] K. S. S. Praveena, E. V. V. Shivaji Ramarao, N. Y. S. Murthy, S. Akkenapally, C. Ganesh Kumar, R. Kapavarapu, *Bioorg. Med. Chem.* **2015**, *25*, 1057.
[15] C. D. Yeo, Y. A. Kim, H. Y. Lee, J. W. Kim, S. J. Kim, S. H. Lee, Y. K. Kim, *Eur. J. Pharmacol.* **2017**, *812*, 189.
[16] C. D. Yeo, J. W. Kim, J. H. Ha, S. J. Kim, S. H. Lee, I. K. Kim, Y. K. Kim, *Exp. Lung Res.* **2014**, *40*, 500.
[17] K. Kelly, A. Mejia, A. N. Suhasini, A. P. Lin, J. Kuhn, A. B. Karnad, S. Weitman, R. C. Aguiar, *Clin. Cancer Res.* **2017**, *23*, 1186.

[18] J. D. Cooney, R. C. Aguiar, *Blood* **2016**, *128*, 2886.
[19] R. Ogawa, M. B. Streiff, A. Bugayenko, G. J. Kato, *Blood* **2002**, *99*, 3390.
[20] P. X. Mouratidis, K. W. Colston, J. B. Bartlett, G. W. Muller, H. W. Man, D. Stirling, A. G. Dalgleish, *Pancreas* **2009**, *38*, 78.
[21] K. Y. Zhang, G. L. Card, Y. Suzuki, D. R. Artis, D. Fong, S. Gillette, D. Hsieh, J. Neiman, B. L. West, C. Zhang, M. V. Milburn, *Mol. Cell.* **2004**, *15*, 279.
[22] S. J. Perry, G. S. Baillie, T. A. Kohout, I. McPhee, M. M. Magiera, K. L. Ang, W. E. Miller, A. J. McLean, M. Conti, M. D. Houslay, R. J. Lefkowitz, *Science* **2002**, *298*, 834.
[23] M. M. Kandeel, H. M. Refaat, A. E. Kassab, I. G. Shahin, T. M. Abdelghany, *Eur. J. Med. Chem.* **2015**, *90*, 620.
[24] M. Fares, S. M. Abou-Seri, H. A. Abdel-Aziz, S. E. Abbas, M. M. Youssef, R. A. Eladwy, *Eur. J. Med. Chem.* **2014**, *83*, 155.
[25] E. Winter, C. D. Pizzol, F. B. Filippin-Monteiro, P. Brondani, A. M. Silva, A. H. Silva, H. G. Bonacorso, M. A. Martins, N. Zanatta, T. B. Creczynski-Pasa, *Chem. Res. Toxicol.* **2014**, *27*, 1040.
[26] L. Provins, B. Christophe, P. Danhaive, J. Dulieu, M. Gillard, L. Quéré, K. Stebbins, *Bioorg. Med. Chem. Lett.* **2007**, *17*, 3077.
[27] J. Senkiv, N. Finiuk, D. Kaminskyy, D. Havrylyuk, M. Wojtyra, I. Kril, A. Gzella, R. Stoika, R. Lesyk, *Eur. J. Med. Chem.* **2016**, *117*, 33.
[28] L. I. Kobylinska, O. Y. Klyuchivska, I. I. Grytsyna, N. Finiuk, R. R. Panchuk, M. O. Starykovych, L. Lehka, R. B. Lesyk, B. S. Zimenkovsky, R. S. Stoika, *Croat. Med. J.* **2017**, *58*, 150.
[29] G. Akalın Ciftci, M. Dilek Altıntop, H. Edip Temel, A. Ozdemir, Z. Asım Kaplancıklı, *Lett. Drug Des. Discov.* **2017**, *14*, 554.
[30] T. A. dos Santos, A. C. da Silva, E. B. Silva, P. A. de Moraes Gomes, J. W. Espíndola, M. V. de Oliveira Cardoso, D. R. Moreira, A. C. Leite, V. R. Pereira, *Biomed. Pharmacother.* **2016**, *31*, 555.
[31] H. He, X. Wang, L. Shi, W. Yin, Z. Yang, H. He, Y. Liang, *Bioorg. Med. Chem. Lett.* **2016**, *26*, 3263.
[32] K. W. Fowler, J. Odingo, *Google Patents*. **2001**.
[33] Q. Y. Lan, Q. L. Liu, J. Cai, A. W. Liu, *Int. J. Clin. Exp. Pathol.* **2015**, *8*, 155.
[34] G. Q. Yu, Z. L. Dou, Z. H. Jia, *Mol. Med. Rep.* **2017**, *15*, 153.
[35] Q. Du, G. Xin, H. Niu, W. Huang, *Mol. Med. Rep.* **2015**, *11*, 4671.
[36] C. Burnouf, M. P. Pruniaux, *Curr. Pharm. Des.* **2002**, *8*, 1255.
[37] M. Boz, S. S. Baştürk, *AOCS* **2016**, *19*, 663.
[38] B. K. Wilk, N. Mwisiya, J. L. Helom, *Google Patents*. **2006**.
[39] S. Kambe, K. Saito, H. Kishi, A. Sakurai, H. Midorikawa, *Synthesis* **1979**, *4*, 287.
[40] L. Y. Ma, L. P. Pang, B. Wang, M. Zhang, B. Hu, D. Q. Xue, K. P. Shao, B. L. Zhang, Y. Liu, E. Zhang, H. M. Liu, *Eur. J. Med. Chem.* **2014**, *86*, 368.
[41] M. M. Mohamed, A. K. Khalil, E. M. Abbass, A. M. El-Naggar, *Synth. Commun.* **2017**, https://doi.org/10.1080/00397911.2017.1332223
[42] M. H. Helal, M. A. Salem, M. S. El-Gaby, M. Aljahdali, *Eur. J. Med. Chem.* **2013**, *65*, 517.
[43] C. Saiz, C. Pizzo, E. Manta, P. Wipf, S. G. Mahler, *Tetrahedron Lett.* **2009**, *50*, 901.
[44] J. L. Marco, N. Martín, A. Martínez-Grau, C. Seoane, A. Albert, F. H. Cano, *Tetrahedron* **1994**, *50*, 3509.
[45] N. Martín, A. Martínez-Grau, C. Seoane, J. L. Marco, A. Albert, F. H. Cano, *Tetrahedron* **1994**, *5*, 1435.
[46] S. Gurumurthi, V. Sundari, R. Valliappan, *Can. J. Chem.* **2009**, *6*, 466.

SUPPORTING INFORMATION

Additional Supporting Information may be found online in the supporting information tab for this article.

How to cite this article: Almatary AM, Elmorsy MA, El Husseiny WM, Selim KB, El-Sayed MA. Design, synthesis, and molecular modeling of heterocyclic bioisostere as potent PDE4 inhibitors. *Arch Pharm Chem Life Sci*. 2018;351: e1700403. https://doi.org/10.1002/ardp.201700403